Spatial and Temporal Variability of Transpiration in the Gwydir and Namoi Catchments from 2000-2004

Stephanie Lyn Weidemann

February 2006

A thesis submitted in partial fulfilment of the requirements for the degree of Master of Environmental Science of the Australian National University

THE AUSTRALIAN NATIONAL UNIVERSITY LIBRARY

This thesis is my own work unless specified by reference.

Signed: 

Stephanie L Weidemann

Acknowledgements

This thesis would not be possible without motivation and support from the following individuals. **Adam Woods**, my love, who has given me energy and endless encouragement. **My family and friends** who have been there for me from the beginning. I would also like to thank:

- **Dr Brendan Mackey** for direction and inspiration;
- **Dr Sandy Berry** for her invaluable assistance and inspire
- **Dr Sue Holzknecht** for her patience, kindness and assistance with the thesis process;

The opportunity to study in Australia as an international student has been a truly amazing and rewarding experience.

Abstract

Vegetation links the atmosphere and the hydrologic cycle. Rapid advances in satellite technology have allowed scientists to monitor changes in vegetation productivity through time. Data from the moderate resolution imaging spectrometer (MODIS) was used to estimate transpiration fluxes in the Gwydir and Namoi catchment areas in northern New South Wales Australia from 6 April 2000 to 31 December 2004. The MODIS NDVI imagery was used to compare differences in gross primary productivity (*GPP*) and to estimate catchment scale transpiration fluxes between croplands and non croplands. Two solar radiation parameters were estimated; daily solar irradiance (R_s) grids were created in ESOCLIM and the global solar irradiance (R_o) using Roderick (1999). These outputs were then used to estimate the diffuse fraction of radiation (R_d/R_s) reaching the vegetation canopy. The fraction of photosynthetic radiation (*fPAR*) was estimated from the MODIS NDVI data. Then the diffuse fraction of radiation was used to yield canopy efficiency (e) (mol CO_2 mol^{-1} PAR). Canopy efficiency and the R_d/R_s were used to estimate GPP using a radiation use efficiency approach. Monthly GPP grids were used to estimate monthly transpiration fluxes from May 2000 to December 2004. Then the monthly transpiration grids were summed to yield annual catchment scale transpiration fluxes from 2001-2004. Temporal estimates of transpiration fluxes display characteristics of wet and dry years. Transpiration fluxes increased with elevation. Vegetation on southerly aspects had higher transpiration rates due to increased radiation received at the surface. Higher annual transpiration fluxes were observed in non cropland pixels and lower annual transpiration fluxes occurred in cropland pixels. Intra-annual and inter-annual patterns of transpiration fluxes were detected from individual pixel analysis. Catchment scale estimates of transpiration fluxes are useful in monitoring the state and productivity of agricultural crops, observing the spatial arrangement of transpiration fluxes across catchments, observing differences in transpiration fluxes for contrasting vegetation types, and monitoring changes in water use efficiency of different vegetation types (e.g. forest versus cropland). Estimates of catchment scale transpiration fluxes have important implications for catchment management in that it provides an explicit functional link between land use/land cover change and catchment-level water budgets.

Table of Contents

List of Figures

List of Tables

Chapter 1: Introduction

Typical of many catchments in Australia's agricultural zone, the Gwydir and Namoi catchments have been heavily modified by clearing native vegetation. The clearing of native vegetation and replacement with agriculture has triggered land degradation problems such as erosion and salinity. These problems can lead to water quality issues and in worst case scenarios health problems. In order to minimize the potential impact of these degradation problems integrated catchment management plans are implemented which require an understanding of the water balance and water quality and how these are affected over time by land use activities. Vegetation plays important roles in the water balance and water quality, and much of the activities prescribed by catchment management plans is focussed on the vegetation cover. Vegetation stores, transports and filters water improving water quality. Critically, plants use water in the process of photosynthesis and this transpiration flux can be a significant component of a catchment's water balance. There is a lack of research involving estimates of transpiration at a catchment scale. Previous studies usually involve estimates from individual plants, or by inference from measuring catchment-level water inputs and outputs.

The aim of this thesis is to investigate an approach to estimating the transpiration flux (i.e. plant-water flux) component of the catchment water balance in the Gwydir and Namoi catchments located in Northern NSW Australia. Estimates of catchment scale transpiration are now possible with real time satellite imagery provided by the Moderate Resolution Spectrometer (MODIS NDVI; see section 2.3.1). New approaches to estimating annual rates of catchment scale transpiration are now possible using MODIS satellite imagery. The approach investigated here is based on a radiation use efficiency model of GPP (Monteith 1972), and then utilises an established relationship between GPP and plant water use (Berry and Roderick 2004). The model of GPP is in turn based upon remotely sensed estimates of vegetation greenness. The available MODIS data enable a time series analysis of the case study catchments at a spatial resolution of 250m, on a q6-day time step from 6 April 2000 to 31 December 2004.

The following section discusses the importance of recognizing how vegetation interacts with the energy and water balances, and provides the essential scientific

background to understand how the MODIS NDVI signal can be used to estimate the transpiration flux at a catchment level.

1.1 Energy and water balance

The relationship between vegetation and the hydrologic cycle is complex. There are numerous interactions that occur. The surface energy balance is linked with water, nutrient and carbon balances (Pielke *et al.*1998). The energy balance includes processes such as canopy resistance, interception of radiation by the canopy and the conversion of solar energy to chemical energy by plants. The radiation use efficiency of photosynthesis (RUE_{Ph}) is the efficiency of photosynthesis in the utilisation of energy. RUE_{Ph} is represented by the following equation (Larcher 2003):

$$RUE_{Ph} = \frac{Stored\ chemical\ energy}{Absorbed\ chemical\ energy}\ 100(\%) \qquad (1)$$

Vegetation links the hydrologic cycle to the atmosphere. The water balance includes processes such as the interception of precipitation by the vegetation canopy, soil water content in the active soil layer, transpiration, evaporation, runoff, stream flow, and water quality. The water balance equation represents the hydrologic cycle as a closed system so that mass or energy is neither lost nor gained (Davie 2003). Here is a simple water balance equation:

$$P \pm E \pm \Delta S \pm Q = 0 \qquad (2)$$

Where P is precipitation, E is evaporation, ΔS is the change in storage, and Q is runoff. Evaporation can be summarised in the following equation (Berry *et al.* 2005):

$$E = E_I + E_S + E_T \qquad (3)$$

Where E is evaporation intercepted from precipitation (I), the soil (S) and through the stomata of plants as transpiration (T). The water use efficiency of photosynthesis (WUE_{Ph}) is the ratio of CO_2 uptake and transpiration. WUE_{Ph} is represented by (Larcher 2003):

$$WUE_{Ph} = \frac{Ph}{Tr}\ (\mu mol\ CO_2\ m^{-2}s^{-1}/mmol\ H_2O\ m^{-2}s^{-1}) \qquad (4)$$

Where *Ph* represents photosynthesis and *Tr* represents transpiration. Vegetation influences all of processes in the hydrologic cycle. The structure of vegetation (e.g. forest versus crop) determines the amount of precipitation intercepted by vegetation. Vegetation structure directs intercepted water from the leaves to the roots where water is stored in the active soil layer. Trees act as funnels capturing water on leaves and directing water flow toward the stem. Intercepted water flows down the stem and sends a pulse of water to the root system. The root system of the plant influences the amount of water in the active soil layer as well as water table levels. In order for plants to use energy for growth, they need water or else the energy stresses the plant and for a plant to utilise energy it needs water otherwise the water infiltrates through the soil or becomes runoff (Stephenson 1990). Water is taken up by plants from the active soil layer and released into the atmosphere via transpiration and evaporation. The stomates on the leaf surface affect the amount of water that is released into the atmosphere and how much atmospheric carbon is absorbed by the leaf. Carbon is acquired at the expense of water loss (Cowan 1982). Stomates receive CO_2 from the atmosphere where it is fixed and then converted to carbohydrates through photosynthesis. Stomatal conductance responds to precipitation, CO_2, solar radiation, soil moisture, air temperature and relative humidity (Pielke *et al.* 1998) Plants have a state which is called optimal stomatal conductance where over one day canopy transpiration is minimised for a fixed amount of total daily photosynthesis (Cowan 1982; Cowan and Farquhar 1977). Plants actively regulate the size of their gas pathway to control the amount of CO_2 and water entering and leaving the leaf surface. *E* above a vegetation canopy is a mixture of transpiration and direct evaporation. The coupling of energy and water balances occurs through transpiration in the canopy, bare soil evaporation, and evaporation of intercepted water from the canopy surface (Silberstein and Sivapalan 1995). Water balance equations can be used to understand the interactions between soil, vegetation and climate on a catchment scale. For example, Farmer *et al.* (2003) used a water balance model to explore the interactions between vegetation, climate and soil on a catchment scale and found that drier catchments were more susceptible to small scale perturbation when compared to humid catchments. Vegetation also influences the amount of runoff to streams by reducing runoff to waterways and acting as filters for sediment which reduces large pulses in stream flow and improves water quality.

There are large variations in the response of catchments to changes in vegetation cover. Deforestation generally causes increases in water yield and decreases in transpiration. Landscape heterogeneity causes horizontal variation in the surface energy budget (canopy resistance) which can affect local and regional precipitation (Pielke *et al.* 1998). The presence or absence of vegetation cover can also affect the microclimate of a catchment. For example, Anthes (1984) suggests that rows of vegetation could induce convective precipitation. See Figure 1.

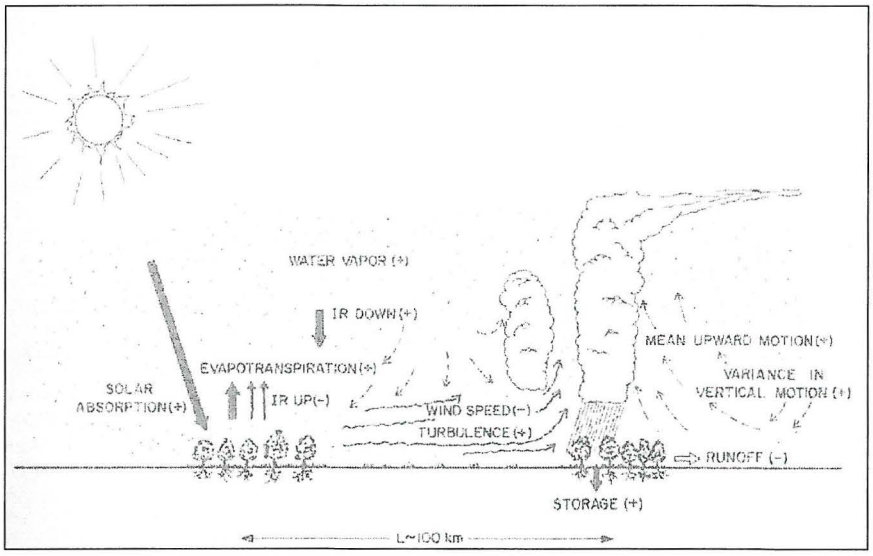

Figure 1. The interactions between vegetation and climate in a semi-arid environment (from Anthes 1984).

Figure 1 shows how vegetation has a direct role in the hydrologic cycle. Vegetation and clouds have a mutual relationship with the water balance. Clouds convert water vapour to liquid water. When water reaches the soil, vegetation then converts the liquid water to water vapour which goes back to the atmosphere (Shukla and Mintz 1982). Evaporation changes with vegetation type. Plants with more leaf to surface area will have higher evaporation and transpiration rates (Zhang *et al.*2001); therefore converting forest to agriculture will reduce evaporation and transpiration rates. Runoff changes with the presence or absence of vegetation. A lack of vegetation cover produces higher runoff events inducing pulses in stream flow. Trees moderate large runoff events and intercept small amounts of water that pass through grasslands (Eldridge and Freudenberger 2005). The absence of vegetation cover results in high rates of sedimentation and increased stream flow (Fohrer *et al.* 2001) which can affect

water quality and aquatic ecosystem integrity. Riparian vegetation or riparian buffer strips act as a filters reducing sedimentation to waterways. Riparian vegetation is vital for aquatic ecosystem integrity and water quality. Along with evaporation, vegetation also affects transpiration.

The transpiration process recycles water between the terrestrial ecosystem and the atmosphere. Temporal estimates of transpiration fluxes over catchments could provide insight into how transpiration fluxes vary with changes in land use and how this affects the water balance. This in turn could provide insight to how much water the canopy is intercepting, how transpiration influences soil water storage and how transpiration affects the amount of runoff. In water-limited environments, plants are sensitive to water availability. Vegetation structure in semiarid environments is mainly controlled by water supply and demand (Kerkhoff *et al.* 2004). Understanding plant water use is an important aspect of understanding the hydrological role of vegetation in the catchment water balance. Estimates of catchment scale transpiration fluxes could provide inputs to catchment water balance models.

Traditional methods of estimating transpiration fluxes involve a bottom up approach by estimating the transpiration flux from single leaves and then scaling up to individual trees. Single leaf estimates of transpiration fluxes involve the complex Penman-Monteith equation for transpiration from a single hypostomatous leaf written as (Thorpe 1978):

$$\lambda E_{leaf} = \frac{sR_{n,\,leaf} + 0.93\rho C_p D / r_b}{s + 0.93\gamma(2 + r_s / r_b)} \tag{5}$$

Where E_{leaf} is the transpiration rate per unit leaf area, $R_{\text{n,leaf}}$ represent the net radiation flux density absorbed by the leaf, ρ is the density, C_p is the specific heat capacity at constant air pressure, λ is the latent heat of vaporisation of water, γ is a psychrometric constant, s is the slope of the saturation vapour pressure curve at ambient air temperature, D is the saturation vapour pressure deficit of air, r_b is the leaf boundary layer resistance and r_s is the stomatal resistance. Transpiration estimates for an individual tree can be found by summing the single leaf transpiration equation over the number of leaves on the tree written as (Zhang *et al.* 1997)

$$\lambda E_{leaf} = L\frac{sR_{n,\,tree} + 0.93\rho C_p D / r_b}{s + 0.93\gamma(2 + \overline{r_s} / r_b)} \tag{6}$$

Where L is the total leaf area of the tree canopy, $\overline{r_s}$ is the measured mean of the stomatal resistance in the tree canopy and $R_{n,tree}$ is the net radiation absorbed per unit leaf area. There are two other conventional methods of measuring transpiration in individual trees. The first method is by measuring stem sap flow by the Compensation Heat Pulse Velocity (CHPV) technique which is based on the stem energy balance. Barradas *et al.* (2005) used the CHPV technique to measure sap flow in young apricot trees while Giorio and Giorio (2003) used the CHPV technique to measure sap flow in olive trees. Barrett *et al.* (1996) used the CHPV technique to measure transpiration of individual trees across a rainforest-eucalypt boundary to see how transpiration rates vary seasonally and between vegetation types. The second technique is the radial fluxmeter method which is based on heat dissipation around a heater probe (Tournebize and Boistard 1998). Wullschleger and Hanson (2005) used the radial fluxmeter method on 24 trees, took hourly measurements in spring from 2000 to 2003 and scaled these values to estimate canopy transpiration in a deciduous forest. This was accomplished using the following equation (Wilson *et al.* 2001):

$$E_{Ci} = J_{Si}A_{Si} / A_G C_i \qquad (7)$$

Where E_{Ci} is the transpiration rate of species i, J_{Si} is the hourly sap flux of the ith species, A_{Si} / A_G is the sapwood to ground area of species I, and C_i is a weighted average of sap flux ratios with depth in the sapwood. Sap flow measurements of transpiration take place on relatively short temporal scales. In order to estimate stand level transpiration individual tree estimates are extrapolated to a stand scale. Wilson *et al.* (2001) found that this scaling up process underestimated transpiration when compared with the soil water budget, catchment water balance and eddy covariance estimates.

Advances in satellite technology have allowed the estimation of large scale vegetation dynamics. This has been accomplished by deriving a Normalised Difference Vegetation Index (NDVI) from the National Oceanic and Atmospheric Association's (NOAA) Advanced Very High Resolution Radiometer (AVHRR) satellite data. Szilagyi (2005) calculated a NDVI from NOAA AVHRR data and compared this with annual transpiration estimates of catchments; annual transpiration was estimated by taking the difference between annual precipitation and runoff. Maselli *et al.* (2004) used AVHRR data as an input to the ecosystem process model FOREST-BGC to

simulate transpiration. Herrmann *et al.* (2005) investigated the spatial and temporal patterns of greenness (NDVI) in the African Sahel from 1982-2003 using NOAA AVHRR satellite data to examine vegetation recovery after drought conditions. In 2000, a new sensor which specialised in monitoring global change dynamics was launched. Data from the MODerate resolution Imaging Spectrometer (MODIS) has been used to observe spatial and temporal vegetation dynamics such as observing seasonal patterns of vegetation growth and dieback (McCloy and Lucht 2004; Beck *et al.* 2005). Currently, transpiration fluxes cannot be estimated directly from satellite data. Instead transpiration is derived from various vegetation parameters.

1.2 Case study catchments

As noted earlier, two catchments in Northern NSW Australia were selected as case studies to investigate the new approach to estimating catchment scale transpiration, namely, the Gwydir and Namoi catchments. Integrated catchment management is an efficient way to manage multiple land degradation issues such as erosion, salinity and water quality in a holistic way. It is important to consider how land is managed because it is crucial to the survival and productivity of vegetation and the survival of organisms. Recently, catchment management has become the focal point for management in the Gwydir and Namoi catchments. Each catchment is managed by a Catchment Management Authority (CMA). CMA's are government bodies that inform communities on the natural resource issues affecting the catchment area. CMA's consider soil, vegetation, water and biodiversity the four indicators of catchment health. The Gwydir catchment is managed under the Border Rivers - Gwydir CMA and the Namoi catchment is managed by the Namoi CMA. CMA's are an important asset to enhancing community understanding of land use change. The following sections briefly describe the current state of the Gwydir and Namoi catchments.

1.3 Gwydir catchment

The natural landscape in the Gwydir catchment has been altered for agriculture. In turn this has affected the productivity potential of the land. The main land degradation issues in the Gwydir catchment include: clearing of native vegetation, exotic plants, soil degradation, increasing dryland salinity, declining riverine ecosystem health and threats to biodiversity. Declining water quality is directly linked to land degradation. Water management issues include degraded riparian areas, agricultural runoff (herbicides and pesticides), salinity, soil erosion, turbidity in lower catchment

waterways and potential eutrophication (Donaldson 1997; DLWC 1999). According to the catchment condition report for the National Land and Water Resources Audit, the Gwydir catchment has poor water condition and poor catchment condition (Walker *et al.* 2001). This is due to land degradation and salinity problems associated with intensive agricultural practices. According to Bradford and Zhang (2002) the Gwydir catchment has experienced a ~61% decrease in forest cover since European settlement. The removal of vegetation can lead to erosion which leads to increased sedimentation. Increased sediment loads carry nutrients to waterways. According to a water quality report by DLWC (2002b), there was an extensive algal bloom in Chaffey Dam near Nundle in 2000-2001 with a peak population of 2 million cells/mL. The Gwydir catchment also has a history of blue-green algal blooms due to high levels of phosphorus from sedimentation (Donaldson 1997). According to Greening Australia (2003a) the central slopes of the Gwydir catchment are some of the most degraded in NSW. The replacement of natural deep rooted vegetation with shallow rooted agricultural land has caused water tables to rise leading to dryland salinity. If native eucalypts are replaced with crops or pasture the water table level will rise because the deep rooted eucalypts that would have tapped into the water supply are gone. Salinity problems can occur when the water table rises and brings up to the surface naturally occurring salts. Saline conditions can cause plants to perish and create areas devoid of vegetation which can be costly to remediate and detrimental to land productivity. Several rivers and streams in the Gwydir and Namoi catchments have been modified with dams and weirs mainly for water supply use and irrigation farming.

1.4 Namoi catchment

The Namoi catchment has also experienced large scale land use change. The main land degradation issues in the Namoi catchment include: clearing of native vegetation, soil degradation, land degradation, increasing dryland salinity, biodiversity decline and water quality decline. The Namoi catchment has undergone a ~54% decrease in forest cover since European settlement (Bradford and Zhang 2002). Some of this forest cover has been replaced by *Pinus radiata* plantations for commercial forestry operations, but the majority of the land has been converted to agricultural land. According to a report by Greening Australia (2003b) the majority of hilly areas in the Namoi have been cleared and contain small amounts of healthy remnant vegetation and riparian areas in the catchment have little or no vegetation (Lampert and Short 2004)

which are considered to be heavily degraded in terms of providing wildlife habitat. Land degradation leads to water quality issues.

Water management issues include: clearing of riparian vegetation, salinisation of freshwater, agricultural runoff to waterways, soil erosion, increased turbidity in streams, and eutrophication (DLWC 2002a). According to the catchment condition report for the National Land and Water Resources Audit, the Namoi catchment has poor water condition and is considered to have poor to almost moderate catchment condition (Walker *et al.* 2001). The Namoi catchment has the most extensive groundwater extraction system in NSW as well as the highest rate of groundwater use in NSW (NCMA 2003). Flows are supplemented during the irrigation season which increases flows and water levels (NSW EPA 1999). Regulated flows disrupt the natural water cycle and ecological integrity of rivers. For example, regulated flows on the Namoi River have caused the disappearance of Red Gum (*E. blakelyi*) communities in some riparian zones. Salinity conditions in the Namoi are an ever increasing problem. The Namoi River is one of the saltiest rivers in New South Wales with some streams saltier than seawater (Namoi CDROM 2000). Pesticide use on farms for disease, pest and weed control can contribute to poor water quality making water unsuitable for drinking and a possible vector for disease which has implications for human health. Pesticide residues are regularly detected between Walgett and Gunnedah (DLWC 2002a) tainting water quality and the ecological integrity of streams. Both catchments are currently experiencing various land management issues. Since these land degradation and water quality issues are interconnected it is imperative to manage them in a systematic way in order to avoid irreversible damage land productivity and ecosystems.

1.5 Thesis Outline

This chapter outlined the scope of the thesis followed by a brief review of how plants interact with the water cycle at the catchment level. The nature of the land management problem in the Gwydir and Namoi catchments were then discussed, including how spatial and temporal estimates of transpiration fluxes can be applied to integrated catchment management.

Chapter 2 outlines the climate, land use and vegetation in the Gwydir and Namoi catchment case studies used in this research, the source data used, and a detailed description of the radiation use efficiency approach used to estimate GPP and transpiration fluxes in the Gwydir and Namoi catchments.

Chapter 3 presents the analysis used to distinguish soil, vegetation and water pixels, as well as the individual pixel analysis for the transpiration fluxes between croplands and non-croplands. This chapter also includes maps of estimated

transpiration fluxes across the Gwydir and Namoi catchments and a comparative vegetation map highlighting croplands in the Gwydir and Namoi catchments. This chapter also discusses the calibration of the fraction of photosynthetically active radiation (fPAR) by distinguishing individual soil, vegetation and water pixels and examines the vegetation parameters used to derive transpiration fluxes in the Gwydir and Namoi catchments. Estimated transpiration fluxes for the Gwydir and Namoi catchments are compared along with the differences in transpiration fluxes between croplands and non croplands.

Chapter 2: Catchment areas, data description and methodology

The MODIS NDVI imagery was used to compare differences in gross primary productivity (*GPP*) and to estimate transpiration fluxes between croplands and non croplands. Two solar radiation parameters were estimated; daily solar irradiance (R_s).and the global solar irradiance (R_o). These outputs were then used to estimate the diffuse fraction of radiation (R_d/R_s) reaching the canopy. The fraction of photosynthetic radiation (*fPAR*) was estimated from the MODIS NDVI images. Then the diffuse fraction of radiation was then used to estimate canopy efficiency (e) (mol CO_2 mol^{-1} PAR). Canopy efficiency and the diffuse fraction of radiation were used in a radiation use efficiency approach to estimate GPP and transpiration fluxes. Annual GPP and transpiration fluxes were then estimated. Differences in annual transpiration fluxes were compared between croplands and non croplands.

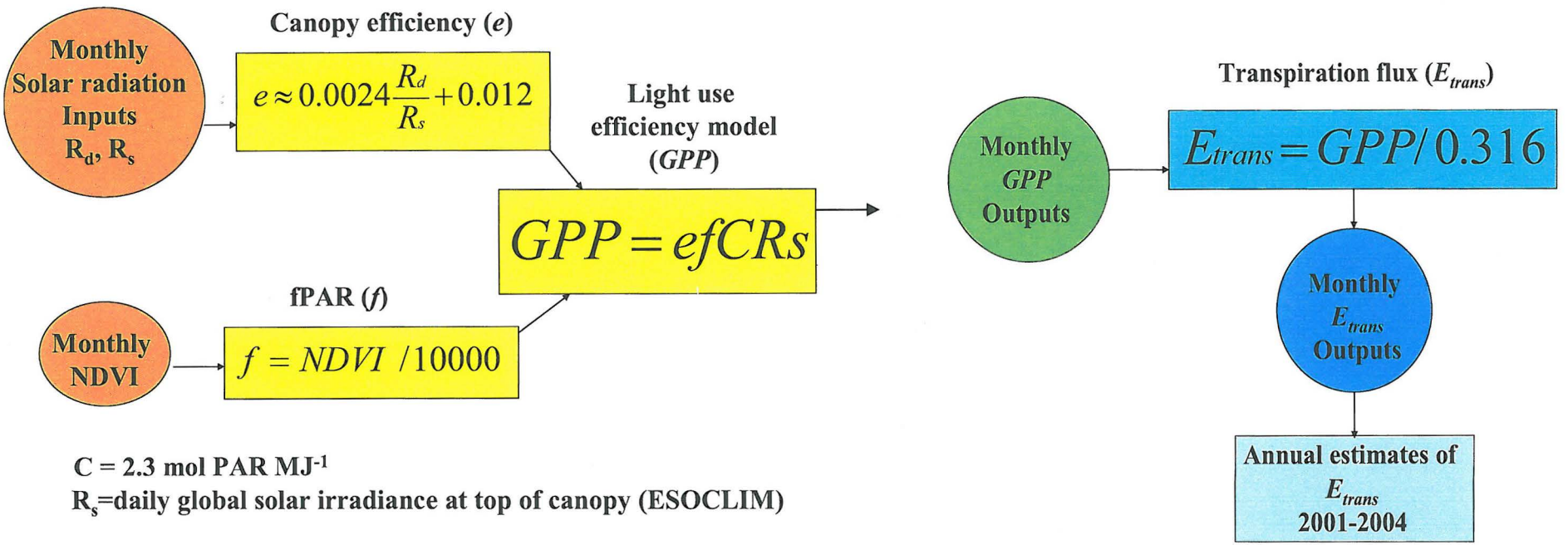

Figure 2. Estimating transpiration fluxes from GPP using a radiation use efficiency approach.

2.1 Study Area

The study area is comprised of the Gwydir and Namoi catchments. Both catchments are located in the Murray-Darling Basin west of the Great Dividing Range in northern NSW, Australia. See Figure 3.

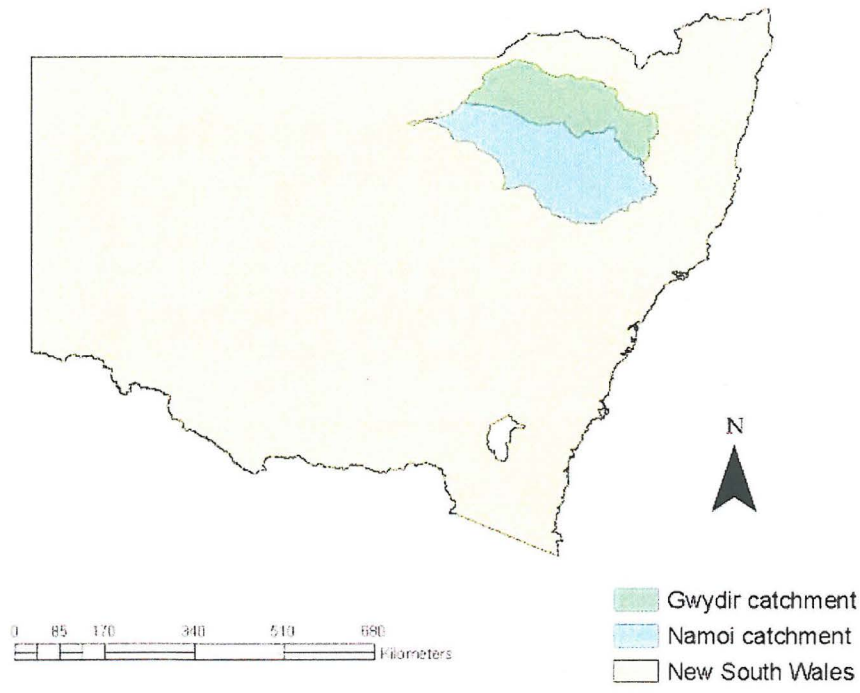

Figure 3. Location of Gwydir and Namoi catchments.

The Gwydir catchment is approximately 26,579km^2 and supports a population of about 25,000 people (AG 2004a). Major towns (from east to west) in the Gwydir catchment include Uralla, Bundarra, Bingara, Warialda and Moree. See Figure 3. The major river that drains the catchment is the Gwydir River. There are two dams on the river: the Kentucky Creek Dam and the Copeton Dam.

The Namoi catchment area is approximately 41,981km^2 supporting a population of about 94,000 people (AG 2004b). The major towns (from east to west) in the Namoi catchment include Tamworth, Werris Creek, Manilla, Barraba, Gunnedah, Narrabri and Walgett (Figure 4). The major river that drains the catchment is the Namoi River. Tributaries drain from the Liverpool Plains in the south, the Nandewar Range in the

north and the Great Dividing Range in the east. There are two dams located on the Namoi River. These are the Split Rock Dam and the Keepit Dam. There are also three dams upstream of the Namoi. These are the Dungowan Dam and the Chaffey Dam on the Peel River and the Quipolly Dam on the Quirindi Creek.

Both catchments are described below based on climate, land use and vegetation. Since European settlement a large portion of native vegetation has been cleared for cropping and grazing. The Interim Biogeographic Regionalisation for Australia (IBRA) divides the continent by distinguished vegetation communities in order to protect the native ecosystems within them. The Gwydir and Namoi catchments span across four IBRA bioregions. From east to west these are the New England Tablelands, Nandewar, Brigalow Belt South, and the Darling Riverine Plains.

2.1.1 Climate

The Gwydir and Namoi catchments experience high rainfall variability. Rainfall comes from the north during summer while low pressure systems and cold fronts come from the south in winter (EPA 1994). Rainfall in the Gwydir catchment falls during summer with ~60% falling between November and March (Donaldson 1997). The mean annual rainfall in the Gwydir catchment is approximately 620mm (Bradford and Zhang 2002). In the eastern tablelands, cold weather during the winter months results in minimal plant growth from late autumn to spring.

In the Namoi catchment, rainfall varies throughout the catchment with an estimated mean rainfall of 491mm in Walgett in the west and 673mm in Tamworth in the east (BOM 2005). The mean annual rainfall across the Namoi catchment is 617mm (Bradford and Zhang 2002). The amount of rainfall generally correlates with longitude (Crapper *et al.* 1997). See Figure 5. The evaporation rates increase from east to west ranging roughly from 1000mm to 1750mm with pan evaporation exceeding the average rainfall across the catchment (Dept of Water Resources, NSW 1992).

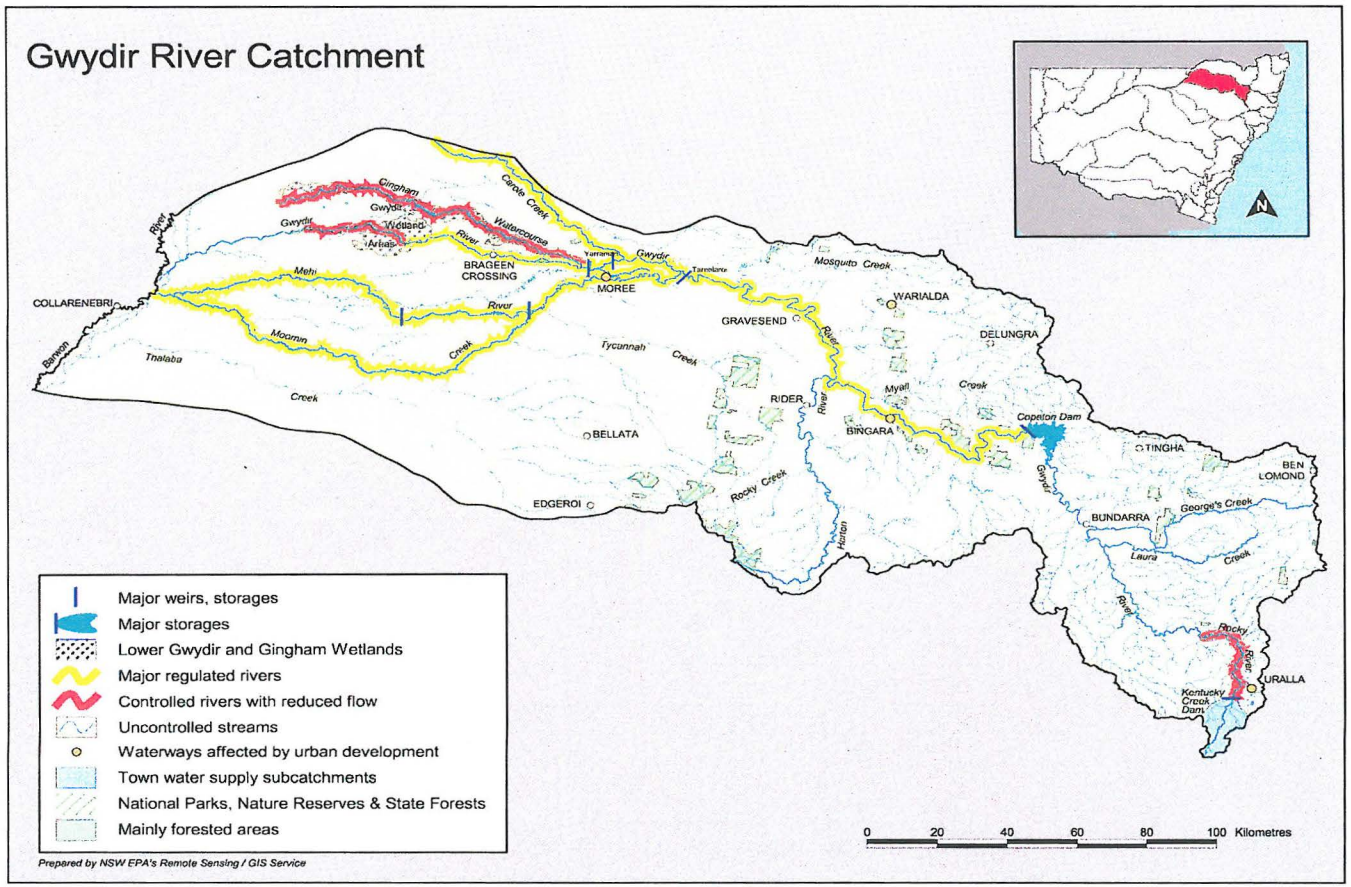

Figure 4. Map of the Gwydir catchment.
(Source: www.epa.nsw.gov.au/ieo/Gwydir/map.htm)

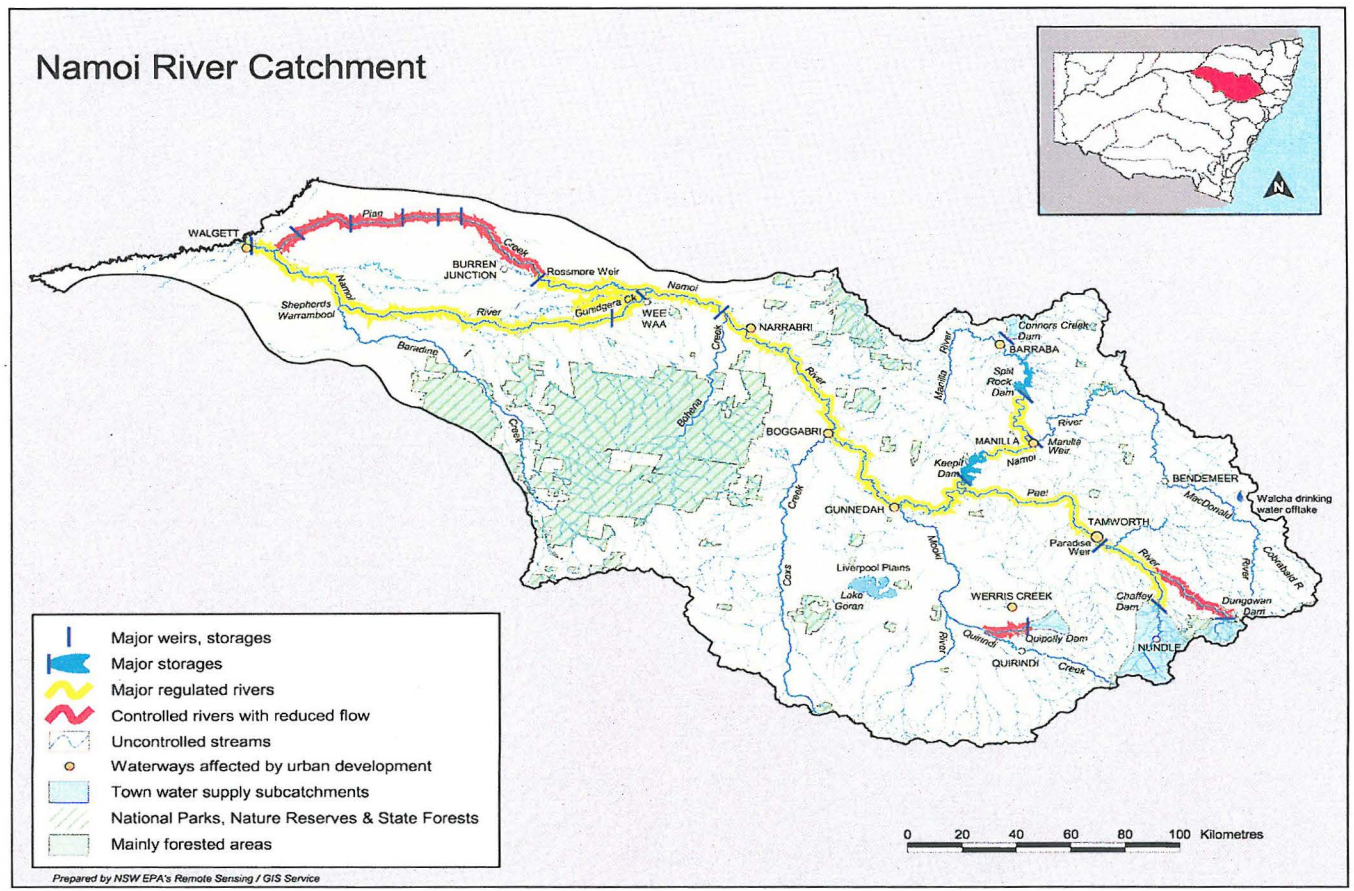

Figure 5. Map of the Namoi catchment.
(**Source**: www.epa.nsw.gov.au/ieo/Namoi/map.htm)

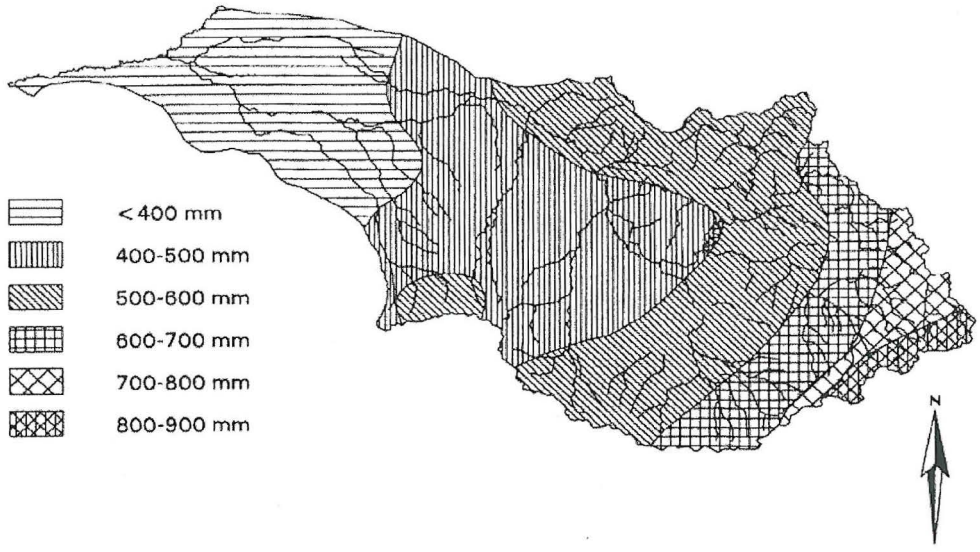

Figure 6. Rainfall map for Namoi catchment (from Crapper *et al.* 1997).

2.1.2 Land use

The majority of land in the Gwydir catchment is used for sheep and cattle grazing. Some of this land has been replaced by *Pinus radiata* plantations for commercial forestry. The Gwydir catchment also hosts the RAMSAR listed Gwydir Valley wetlands. The main land uses in the Namoi catchment include forestry, croplands (cotton, cereals, pulses and oilseeds), pasture, grazing, dryland and irrigated agriculture. Native or improved pasture occupies 20860 km^2, followed by timber with 10545 km^2, cropping including grain, fibre and fodder with 9813 km^2, irrigation with 828 km^2, urban land with 85 km^2, water at 84 km^2 and surface mining, rock outcrops and roads with 32 km^2. Cotton is the largest agricultural industry in the Namoi catchment which is worth ~$1 billion annually.

2.1.3 Native vegetation - Gwydir catchment

This section summaries the vegetation in the Gwydir catchment starting with the tablelands in the east and finishing in the Darling Riverine Plains in the west. The New England Tablelands comprise a mixture of steep terrain along with undulating hills. The steep terrain is dominated by Red Stringybark (*R. macroryhncha*) while the hilly areas have been cleared for grazing and contain little native vegetation (Greening Australia, 2003a). The Nandewar region contains croplands in the valley and hilly areas with White Cypress Pine (*Callitris hugelli*) or Ironbarks. The Brigalow region is mainly dryland cropping with few areas of native remnant vegetation remaining. Some

areas in the central catchment contain commercial forestry plantations of *Pinus radiata*. In the western region the Darling Riverine Plains provide water for irrigation farming. There are a few highly degraded remnant areas of Poplar Box woodland and the Coolibah Black Box woodland which have recently been listed as an endangered vegetation community (NPWS 2004). The Gwydir catchment hosts three nationally listed ecological communities. These are Brigalow (*Acacia harpophylla*), Grassy White Box Woodlands (*E. albens*) and Semi-Evergreen Vine Thicket (GCMB 2003). In addition to this the Gwydir catchment also hosts the RAMSAR listed Gwydir wetlands which are located on privately owned land 60km west of Moree covering approximately 8.23km^2. These wetlands are an ecologically imperative for the survival of thousands of migratory and nomadic birds that breed in the wetlands every year. Unfortunately portions of the Gwydir and Gingham watercourses are regulated and have reduced flows which are directly affecting water availability in the wetlands and changing the composition of the vegetation communities.

2.1.4 Native vegetation – Namoi catchment

The following section is a summary of the major vegetation communities found in the Namoi catchment starting with the higher elevations in the east and extending to the Liverpool plains in the west. The Peel River subcatchment contains wet sclerophyll forests that are dominated by Brown Barrel (*E. fastigata*), Messmate (*E. oblique*) and Manna Gum (*E. viminalis*). There are also scattered communities of Red stringybark (*E. macrorhyncha*), White box (*E. albens*) and Yellow Box (*E. melliodora*). Blakelyi's Red Gum (*E. blakelyi*) is present along riparian corridors, but is disappearing due to altered hydrologic regimes from agriculture (i.e. irrigation). Most rivers are dominated by River Oak (*Casuarina cunninghamiana*). In the MacDonald and Manilla subcatchments Messmate, Red Stringybark, Manna Gum and Black Sallee (*E. stellulata*) are present along with White Box Woodlands and Savannah Woodland communities. The Mooki subcatchment hosts Grey Box, White Box, Yellow Box and a Blakely's Red Gum community as well as a Plains Grass community (*Stipa aristiglumis*). There are also White Box and Cypress Pine communities. The middle Namoi River subcatchment contains Yellow Box, White Box and Bimble Box (*E. populnea*) along with a White Cypress Pine community in the Pilliga sandstone. *Pinus radiata* commercial forestry plantations are scattered throughout the central and western catchments. The lower Namoi subcatchment contains the Pilliga Scrub which is a large part of the Brigalow Belt South bioregion (500,000+ hectares). The Pilliga Scrub is the

largest remaining area of continuous semi-arid woodland in the temperate climate of eastern Australia. The dominant species found in this region include: White Cypress Pine, Narrow-leaved Ironbark (*E. creba*), Brown Bloodwood (*E. trachyphoia*), Blakely's Red Gum, Pilliga Box (*E. pilligaensis*) and Bull oak (*Casuarina leuhmannii*). There are also some Coolibah (*E. coolabah*) Woodlands and grasslands dominated by Mitchell grass or Plains grass (*Astrebla lappacea*).

2.2 Data description

2.2.1 MODIS

The data used in this research originates from the MODIS sensor onboard the National Aeronautic Space Administration's (NASA) Terra satellite. This satellite was launched on 18 December 1999 as part of NASA's Earth Observing System (EOS). MODIS satellite data is used by a variety of scientists to enhance knowledge in global change dynamics. For example, MODIS can measure the photosynthetic activity of land and marine plants to yield more accurate estimates of how much greenhouse gases are being absorbed and used in plant productivity by time series analysis of satellite imagery. It can also track seasonal and inter-annual changes in plant activity. MODIS tracks a wider array of Earth's vital signs than other sensors with a viewing swath of 2330km and 36 spectral bands ranging from 0.4μm to 14.4μm at three resolutions: 250m, 500m and 1000m (MODIS, 2005). MODIS has a two day repeat coverage of the Earth's surface at an altitude of 705km therefore data can be monitored on various temporal scales (i.e. weekly, monthly, and annually).

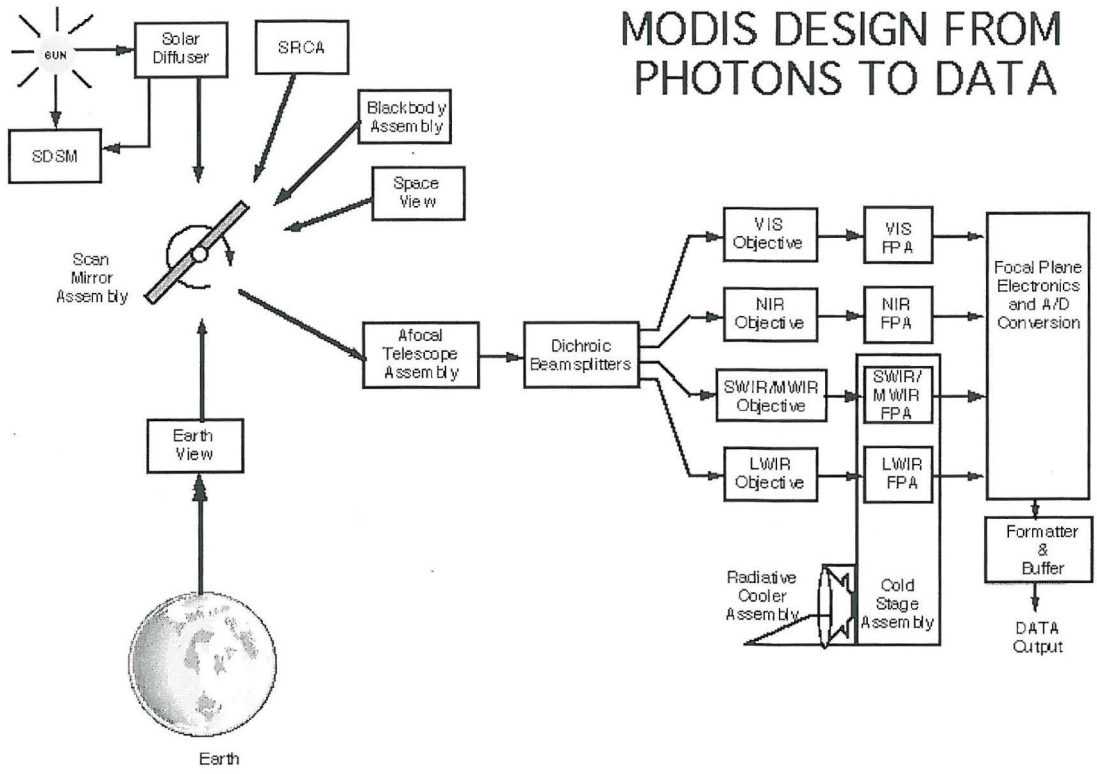

Figure 7. How MODIS converts light energy to digitized land surface data; specifically, the sensor captures the energy reflected/emitted from Earth's surface and calculates the NDVI from a normalised index of the red and near-infrared bands.

(**Source:** http://www.mcst.ssai.biz/mcstweb/calib/spectral.html)

Figure 7 displays the process of how the MODIS sensor converts light energy and Earth's landscape into remotely sensed data. Band 1 data from the MODIS sensor is used in this study. It specialises in measuring the photosynthetic activity of plants through the NDVI.

2.2.2 NDVI

NDVI is a measure of green leaf density or the density of chloroplasts within the leaves. NDVI is an indicator of vegetation conditions and is used in estimating large scale terrestrial ecosystem productivity. NDVI is represented in the following equation (MODIS 2006):

$$NDVI = \frac{\alpha_{0.86\mu m} - \alpha_{0.67\mu m}}{\alpha_{0.86\mu m} + \alpha_{0.67\mu m}} \qquad (8)$$

This equation symbolizes the ratio of albedos (α) at different wavelengths. Chlorophyll pigments in leaves absorb visible radiation (400-700nm) and reflect near infrared radiation (0.7-5μm). Green leaves typically absorb more than 85% of the solar radiation in the visible wavelength and less than 50% of light in the near-infrared wavelength (Bonan 2002). The NDVI is a widely used index in remote sensing studies to monitor vegetation dynamics over large spatial scales. The NDVI allows the comparison of seasonal and inter-annual variability of vegetation growth and activity. NDVI data provides spatial detail on the timing of active growing seasons (Myneni *et al.* 1997). Higher NDVI values indicate more greenness or increased vegetation productivity. Generally green vegetation will have a positive NDVI, soil has a NDVI value approaching 0 and water will have a negative NDVI, but this varies throughout the landscape. Tucker *et al.* (1986) found values of -0.2μm to 0.05μm for snow, inland water, deserts and exposed soils and 0.05μm to 0.7μm for green vegetation. The MODIS data displays the actual NDVI values of the landscape.

2.3 Data sources

2.3.1 MODIS NDVI

The satellite data used in this study is MODIS band 1 data acquired from the ANU archive of MODIS data in the School of Resources, Environment and Society. This data was downloaded from the MODIS web data products page at http://modis.gsfc.nasa.gov/data/dataprod/index.php. The imagery starts on 6 April 2000 and goes through to 31 December 2004. Each image has a spatial resolution of 250m. The Charles Sturt University webpage (http://life.csu.edu.au/geo/findlatlong.html) was used to determine the latitude and longitude coordinates surrounding the Namoi and Gwydir catchments.

Dr. Sandy Berry extracted the following coordinates (28°S to 32°S and 146°E to 154°E) from continental Australia MODIS data. She created five images in ERDAS Imagine; one image for each year from 2000-2004. The year 2000 has 17 layers – one layer per month from April to December and from 2001 to 2004 there are 23 layers each from January to December. Each MODIS band 1 layer shows the greenness indices or the NDVI in a 16 day composite. The brightest pixel out of each 16 day period (layer) is displayed. In total there are 109 layers. See Table 1 and Table 2 for MODIS layer details.

Table 1. Time period for MODIS layers for the year 2000: 16 day composites.

Layer #	Time period
1	6 APR - 21 APR
2	22 APR - 7 MAY
3	8 MAY - 23 MAY
4	24 MAY - 8 JUNE
5	9 JUNE - 24 JUNE
6	25 JUNE - 10 JULY
7	11 JULY - 26 JULY
8	27 JULY - 11 AUG
9	12 AUG - 27 AUG
10	28 AUG - 12 SEPT
11	13 SEPT - 28 SEPT
12	29 SEPT - 14 OCT
13	15 OCT - 30 OCT
14	31 OCT - 15 NOV
15	16 NOV - 1 DEC
16	2 DEC - 17 DEC
17	18 DEC - 31 DEC

Table 2. Time period for MODIS layers for years 2001 to 2004: 16 day composites.

Layer #	Time period
1	01 JAN - 16 JAN
2	17 JAN - 01 FEB
3	02 FEB - 17 FEB
4	18 FEB - 05 MAR
5	06 MAR - 21 MAR
6	22 MAR - 06 APR
7	07 APR - 22 APR
8	23 APR - 08 MAY
9	09 MAY - 24 MAY
10	25 MAY - 09 JUNE
11	10 JUNE - 25 JUNE
12	26 JUNE - 11 JULY
13	12 JULY - 27 JULY
14	28 JULY - 12 AUG
15	13 AUG - 28 AUG
16	29 AUG - 13 SEPT
17	14 SEPT - 29 SEPT
18	30 SEPT - 15 OCT
19	16 OCT - 31 OCT
20	1 NOV - 16 NOV
21	17 NOV - 2 DEC
22	2 DEC - 18 DEC
23	19 DEC - 31 DEC

2.3.2 Solar radiation data

The solar radiation data involves the estimation of two variables. These are the global solar radiation at the surface (R_s) and the solar radiation received at the top of the atmosphere (R_o). R_s was estimated in ESOCLIM which is part of the ANUCLIM 5.1 software package (Centre for Resource and Environmental Studies, ANU). This program estimates mean monthly climate values and creates climate surfaces. The digital elevation model (DEM) was the input for this model. 56 monthly output grids were created (May 2000-December 2004). R_o surfaces were estimated by Dr Sandy Berry using Table 5 in Roderick (1999). The units for both surfaces are in MJ m^{-2} day^{-1}.

2.3.3 Vegetation data

The vegetation dataset used in this research was downloaded from the Geoscience Australia website (http://www.ga.gov.au) titled *Vegetation - Post-European Settlement (1988)*. This dataset was digitized from Carnahan's AUSLIG vegetation map (1:5,000,000 map scale). The spatial extent of the data is -9.0°N, -44.0°S, 112.0°W and 154.0°E. The vegetation data is classified based on the (a) tallest stratum species dominant (ts_td), (b) tallest stratum species co-dominant (ts_sc), (c) tallest stratum growth form (ts_gf) and (d) tallest stratum density of foliage cover (ts_d). Understory vegetation types are also included.

2.4 Estimation of GPP

GPP is the rate at which a plant fixes carbon. In order for a plant to absorb atmospheric carbon the stomata need to be open and the plant must have access to water. Stomata open in the morning and close in the evening in response to light intensity. Stomata have a major influence on the rate of transpiration and gas exchange across the leaf surface. When stomata are closed this averts the loss of water vapour and promotes the absorption of CO_2. CO_2 is a vital part of photosynthesis. Transpiration is linked to the uptake of CO_2. In order for the diffusion of CO_2 to occur the leaf surface must be moist. The moist leaf surface converts the atmospheric carbon into a solution which is then absorbed by the plasma membrane. In water-limited environments, the vegetation canopy optimizes the uptake of atmospheric carbon depending on the amount of available water. Cowan and Farquhar (1977) proposed a theory of optimal stomatal conductance where canopy transpiration is minimised for a fixed amount of total daily photosynthesis. GPP was estimated by using a radiation use

efficiency approach (Roderick *et al.* 2001) using the Monteith (1972) light use efficiency model:

$$GPP = efCR_s \quad (9)$$

Where *GPP* is the daily net assimilation rate of the canopy (mol CO_2 m^{-2} $month^{-1}$), *e* is the canopy efficiency (mol CO_2 mol^{-1} PAR), *f* is the fraction of photosynthetically active radiation (fPAR), *C* is a constant (2.3 mol PAR MJ^{-1}) used to convert from global solar irradiance to quanta in the PAR part of the spectrum and R_s is the daily global solar irradiance at the top of the canopy. In order to estimate the GPP, the diffuse fraction of radiation and the canopy efficiency were estimated in IDRISI first (Berry and Roderick 2004).

2.4.1 Monthly NDVI estimates

Monthly NDVI estimates were calculated from the MODIS data using a method devised by Dr. Berry (pers. comm.) shown below. Images are depicted by (*I*) in front of the image number (e.g. I2 is image 2).

$$\overline{NDVI}_1 = (16 * I1 + 15 * I2) / 31$$

$$\overline{NDVI}_2 = (1 * I2 + 16 * I3 + 11 * I4) / 28$$

$$\overline{NDVI}_3 = (5 * I4 + 16 * I5 + 10 * I6) / 31$$

$$\overline{NDVI}_4 = (6 * I6 + 16 * I7(I1) + 8 * I8(I2)) / 30$$

$$\overline{NDVI}_5 = (8 * I8(I2) + 16 * I9(I3) + 7 * I10(I4)) / 31$$

$$\overline{NDVI}_6 = (9 * I10(I4) + 16 * I11(I5) + 5 * I12(I6)) / 30$$

$$\overline{NDVI}_7 = (11 * I12(I6) + 16 * I13(I7) + 6 * I14(I8)) / 31$$

$$\overline{NDVI}_8 = (12 * I14(I8) + 16 * I15(I9) + 3 * I16(I10) / 31$$

$$\overline{NDVI}_9 = (13 * I16(I10) + 16 * I17(I11) + 1 * I18(I12))/ 30$$

$$\overline{NDVI}_{10} = (15 * I18(I12) + I19(I13) / 31$$

$$\overline{NDVI}_{11} = (16 * I20(I14) + 14 * I21(I15)) / 30$$

$$\overline{NDVI}_{12} = (2 * I21(I15) + 16 * I22(I16) + 13 * I23(I17)) / 31$$

*images listed in red are year 2000 images

The monthly NDVI estimates were calculated using the map calculator in IDRISI Kilimanjaro. One grid was created for each month. Eight grids were created for the year 2000 for months May to December and 12 grids for the years 2001 to 2004 for months January to December. In total 56 grids were created.

2.4.2 Calibrating fPAR

The NDVI has been hypothetically and empirically related to the fPAR absorbed by vegetation canopies (Kumar and Monteith 1982; Sellers 1985; Sellers 1987; Veroustraete *et al.* 1996; Justice *et al.* 1998; Fensholt *et al.* 2004), thus the fPAR can be estimated from the NDVI surfaces. fPAR is the fraction of photosynthetically active radiation (0.4-0.7μm) intercepted by the sunlit vegetation. A visual analysis of the MODIS imagery was undertaken in order to distinguish soil and vegetation pixels. After adjusting the colour display soil pixels appeared brown and vegetation pixels appeared various shades of green. MODIS imagery is essentially a photograph of the landscape at a 250m resolution. Green vegetation and bare soil patches are evident (colour contrast). The NDVI values range from -0.3 to 1 and the fPAR values range between 0 and ~0.95. A pixel with a NDVI of 0 was assumed to have a fPAR of ~0.17. A pixel with a NDVI of 1 was assumed to have a fPAR of ~0.95. See Figure 7 for the relationship between fPAR and NDVI.

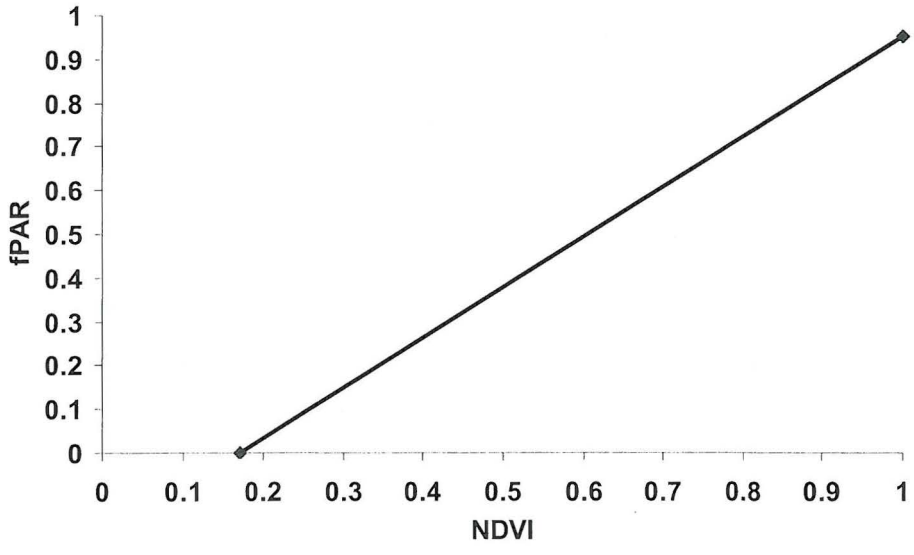

Figure 8. The relationship between NDVI and fPAR.

In order to calibrate fPAR, nine pixels were chosen at random to compare their spectral signatures. By viewing the MODIS imagery in IDRISI Kilimanjaro, three pixels assumed to represent soil (brown), three pixels assumed to represent productive vegetation (bright green) and three pixels assumed to represent water (blue) were chosen.

The canopy efficiency (e) is the rate at which the vegetation canopy photosynthesizes per unit radiation absorbed. Canopy efficiency was estimated by using the Roderick *et al.* (2001) equation below:

$$e \approx 0.024\frac{R_d}{R_s} + 0.012 \tag{10}$$

Where e is the canopy efficiency and R_d/R_s is the diffuse fraction of radiation. The canopy efficiency grids were created in monthly intervals. In total 12 grids were created. The grids were calculated using the diffuse fraction of radiation as inputs into the map calculator in IDRISI. The output grids were then multiplied using the radiation use efficiency model described above: canopy efficiency (e), fPAR (f), solar constant (C) and the global solar radiation at the surface (R_s).

The diffuse fraction of radiation R_d/R_s was estimated using the following equation (Roderick *et al.* 2001):

$$\frac{R_d}{R_s} = 1.11 - 1.31 * \left(\frac{R_s}{R_o}\right) \tag{11}$$

Where, R_d is the solar irradiance at the top of the vegetation canopy, R_s is the global solar irradiance at the surface and R_o is the solar radiation received at the top of the atmosphere. R_s/R_o represents the atmospheric transmission or the clearness index (Roderick 1999). R_s was created by using ESOCLIM. R_o was calculated from Roderick (1999). The diffuse fraction was calculated using the IDRISI Kilimanjaro map calculator and estimated for each month. In total 56 grids were created. Twelve grids for each year from 2001-2004 were summed to yield annual GPP estimates.

2.5 Estimating transpiration fluxes

Transpiration cannot be estimated from remotely sensed data directly. However, other relevant vegetation parameters can be measured directly that can be used to estimate transpiration. Transpiration is water loss from a plant surface. This occurs as the vaporization of water through the stomata of plants (Brutsaert 1982) when the vapour pressure in the leaf cells is greater than the atmospheric vapour pressure (Barry and Chorley 1998). Water loss from leaves is controlled by day length, leaf temperature, surface area, tree species, age, available energy, atmospheric vapour pressure and wind speed. It also depends on the size of the stomatal openings which varies with environmental conditions, available energy and atmospheric conditions. Other factors affecting transpiration are net radiation, aspect, stomatal resistance, canopy resistance, the saturation deficit (McNaughton and Jarvis 1983), available soil water and the plant's ability to transfer water from the soil to its leaves (Davie 2003). Transpiration is not a waste product of the plant, but rather a necessary mechanism so the plant can absorb atmospheric carbon. The mesophyll cells within the stomata need to be saturated for the plant to absorb carbon from the atmosphere while the stomata are open. In this thesis the transpiration flux was estimated using an equation adapted from Berry and Roderick (2004) which relates CO_2 uptake to the transpiration flux. Here we assume that GPP, transpiration and atmospheric CO_2 are directly proportional to each other. See equation below:

$$E_{trans} = GPP / 0.316 \qquad (12)$$

Where, E_{trans} (kg m^{-2} $month^{-1}$) is the transpiration flux and GPP (mol CO_2 m^{-2} $month^{-1}$) is the gross primary productivity. The transpiration fluxes were estimated for each month from January through to December using the IDRISI map calculator. This was accomplished by dividing the monthly GPP grids created above by

0.316kg H_2O mol^{-1} CO_2. In total 56 grids were created. Then, twelve grids from each year (2001-2004) were summed to yield annual transpiration fluxes.

2.6 Estimating transpiration fluxes for different land cover types

2.6.1 Descriptive statistics

Descriptive statistics were calculated to extract croplands from non croplands. The mean, variance, standard deviation and coefficient of variation were calculated using the monthly fPAR grids created in IDRISI. The mean for each monthly fPAR image was calculated using the IDRISI map calculator. All January images from 2001 to 2004 were summed and divided by four. This resulted in the mean fPAR for each month from January to December (2001-2004). See formula below (Sokal and Rohlf 1995):

$$\overline{Y} = \frac{\sum Y}{n} \tag{13}$$

Where Y represents each month, n represents the sum of all n items. The variance was calculated by using the monthly mean fPAR grids, squaring them and dividing by 12 (12 grids total). See formula below (Sokal and Rohlf 1995):

$$Variance = \frac{\sum y^2}{n} \tag{14}$$

Where y is the monthly fPAR grid and n is the number of grids. The standard deviation was calculated by taking the square root of the variance fPAR grids. See formula below (Sokal and Rohlf 1995):

$$s = +\sqrt{\frac{\sum y^2}{n}} \tag{15}$$

The coefficient of variation (COV) was calculated by multiplying the standard deviation grids by 100 and dividing them by the mean fPAR grids. See formula below (Sokal and Rohlf 1995):

$$COV = \frac{s \times 100}{\overline{Y}} \tag{16}$$

The COV is the standard deviation expressed as a percentage of the mean.

2.6.2 Distinguishing croplands and non croplands

To observe oscillations in the transpiration flux through time at the individual pixel scale, eight pixels were chosen from the COV images based on their values using IDRISI. Cropland pixels displayed high COV values while non cropland pixels displayed low COV values. GPP and transpiration flux values were extracted for each catchment. Pixel locations were recorded in columns and rows and labelled *a*, *b*, *c*, *d*, *e*, *f*, *g* and *h*. Four cropland pixels were chosen and these pixels were labelled *a*, *b*, *c* and *d*. Then four non-cropland pixels were chosen, these were labelled *e*, *f*, *g* and *h*. An IDL program (v. 5.6) was used to create a pixel drill. This program picked the same pixel out of every image based on the pixel coordinates. The program was compiled and run to acquire the transpiration flux values for the eight pixels. The pixel drill was run through all 56 monthly transpiration images from 2000 to 2004.

Cropland pixels were extracted in each catchment using IDRISI. All other pixels were classifieds as non-croplands. Water was masked and three classes were created (croplands, non-croplands, and water). Summary statistics for annual GPP and annual transpiration flux for years 2001-2004 were calculated separately for each catchment in IDRISI. These statistics included the total GPP and transpiration for each year from 2001 through 2004 along with GPP and transpiration estimates of pixels containing croplands and non-croplands. The total area of each catchment and the areas of cropland and non cropland pixels were also calculated. The Carnahan's AUSLIG vegetation dataset was then compared to the cropland and non cropland vectors extracted from the transpiration grids as an independent land cover data source.

Chapter 3: Results and Discussion

Prior to analysing catchment scale data, individual pixels were classified into soil, vegetation and water based on spectral signatures (Section 3.1) in order to calibrate fPAR from NDVI data. This was followed by calculating the descriptive statistics for each year to distinguish croplands and non croplands on a catchment scale (Section 3.2). By using fPAR, NDVI and GPP data, catchment scale transpiration can be estimated. Individual pixel analysis of the annual transpiration grids allowed the comparison of transpiration fluxes between croplands and non croplands (Section 3.2.2). Catchment scale transpiration fluxes were then estimated annually (Section 3.2.3). Then the MODIS data was compared to Carnahan's vegetation dataset to check accuracy of the descriptive statistics calculations (Section 3.3).

3.1 Spectral signatures of individual pixels

Preliminary spectral analysis of the satellite data involved choosing three pixels for three different land use cover (soil, vegetation and water) to see how pixel NDVI values varied through time. This was accomplished by analysing the MODIS NDVI imagery in IDRISI and selecting pixels that displayed characteristics of soil, vegetation and water. These pixels were chosen based on their NDVI values. Inherently, pixels will be covered with a mixture of soil and vegetation causing the NDVI values to fluctuate. The NDVI values range from -0.3 to 1.0. When NDVI is equal to 1.0 it is assumed that the pixel is covered completely by green vegetation and the fPAR that is intercepted by the canopy is ~0.95 and when the NDVI is less than or equal to 0.17, the fPAR is equal to 0. (S. Berry pers. Comm..24 November 2005). When a pixel includes a mixture of green vegetation and water the fPAR is underestimated due to the reflective properties of the water. This distorts the spectral signature of the pixel by increasing reflective noise in the data. Figures 9 through 11 display the same soil, vegetation or water pixel through the 109 MODIS images from April 2000 to December 2004. For individual pixel analysis, it is assumed that a pixel with high NDVI values contain productive vegetation. There are visible changes in greenness amounts annually and seasonally. For example, growing seasons can be distinguished in the soil pixels (Figure 9).

3.1.1 Spectral signatures of soil pixels

The spectral signatures for three soil pixels are shown below in Figure 9.

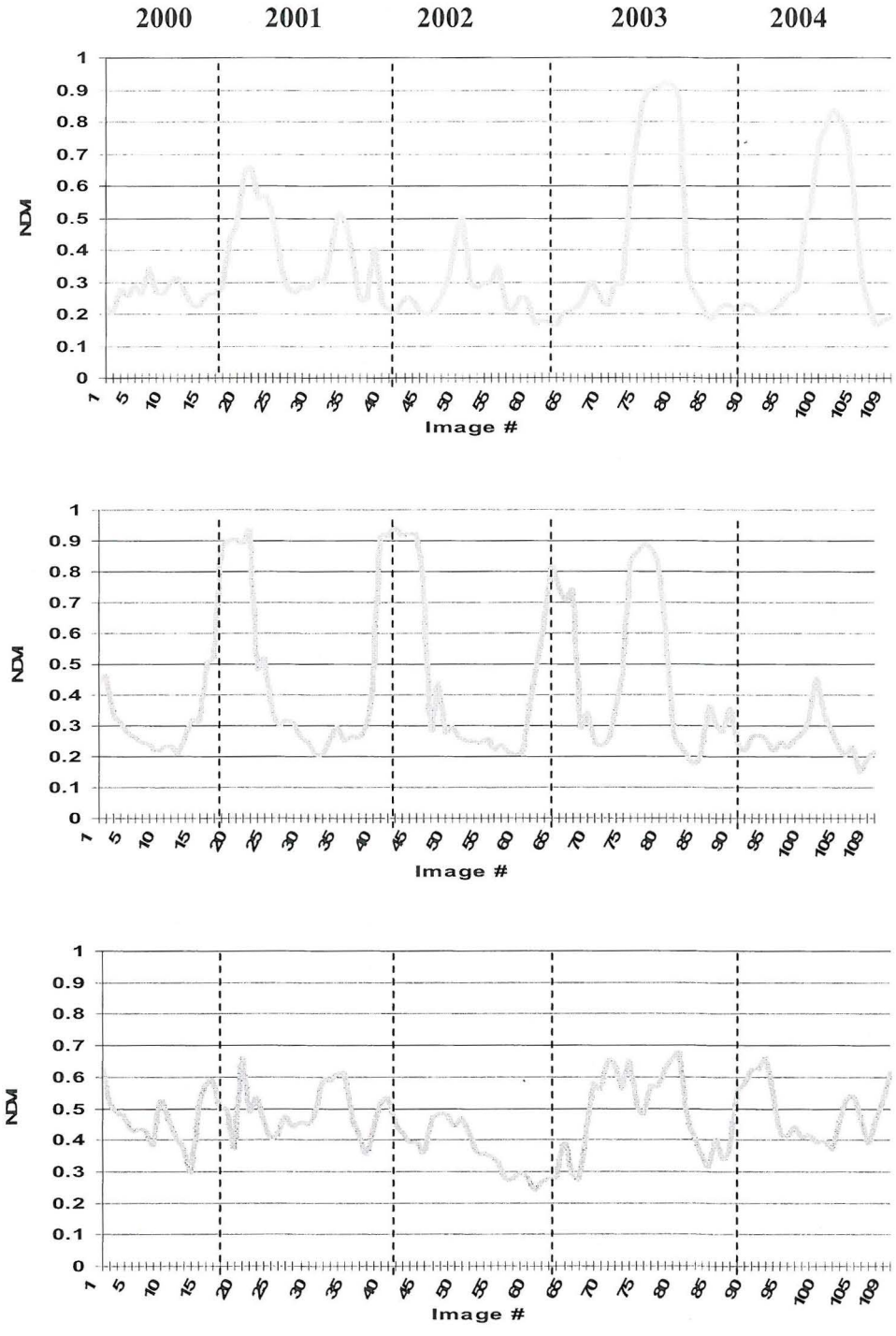

Figure 9. NDVI values of three pixels assumed to contain soil.

Figure 9 shows the comparison of the soil spectral signatures. The first two soil pixels in Figure 9 display characteristics of crop pixels. This is apparent in the pattern of the spectral signatures for individual pixels. There are noticeable peaks and troughs

in the NDVI values, suggesting that there are rapid growth spurts in plants due to rapid increases in greenness values. There are also rapid decreases in greenness values denoting the bare soil after crop harvest.

In the first soil pixel there are two major peaks of greenness. These peaks represent increases in NDVI in this pixel. These peaks are evident in images 78 and 101. These images have NDVI values of 0.92 and 0.84 respectively which depicts productive vegetation. There are large decreases in NDVI values with minimum NDVI values occurring in images 84 and 107. These images have NDVI values of 0.18 and 0.17 which depicts bare soil. According to the MODIS timeline these peaks of greenness occurred between August 2003 (image 78) and November 2003 (image 84) as well as August 2004 (image 101) to November 2004 (image 107). The growing seasons for these pixels began at the end of winter through the end of spring. The smaller peaks suggest years of poor crop growth. The highest NDVI value for the minor peaks of greenness from 2000 to 2002 was 0.64. These years were clearly not as successful for crop growth as 2003 and 2004 where the highest NDVI values were 0.92 and 0.84.

The second soil pixel spectral signature shows a typical crop pixel pattern with sharp increases in NDVI, a NDVI plateau for a few images during peak crop growth and then a sharp decrease in NDVI after crop harvest. The second soil pixel displays four major peaks of greenness. The first peak begins in March 2001 (image 21) with an NDVI value of 0.93, and then decreases rapidly in August 2001 (image 31) with a minimum NDVI value of 0.21. The second peak has a maximum NDVI value of 0.94 which occurred in the middle of summer in January 2002 (image 41) and had a minimum NDVI value of 0.21 which occurred in October 2002 (image 58). The third peak has a maximum NDVI value of 0.82 which occurred during January 2003 (image 63) and had a minimum NDVI value of 0.24 (image 70) during April 2003. The fourth peak has a maximum NDVI value of 0.89 which occurred during August 2003 (image 76). The minimum NDVI value for this pixel was 0.18 (image 83) which occurred during November 2003. The maximum NDVI value of 0.94 (image 41) occurred in January 2002. The second crop pixel experiences different growing seasons than the first crop pixel. The first peak occurs at the end of autumn and over winter. Years 2000 and 2001 were the wettest years out of the five years. This could influence the late growth indicated in this pixel. The second peak of growth is also delayed; this is due to the delay in the first crop growing season. The third and fourth peaks occurred during a shorter time period than the first two peaks. The third peak occurred during the middle

of summer 2002 to early autumn 2003. This time period was the driest out of the five years, therefore, this growing season must have been heavily irrigated. The fourth greenness peak coincides with the growing seasons in the first soil pixel (August to November).

The third soil pixel displays a spectral signature that is quite different from the other soil pixels in that there are no defined peaks of greenness. The minimum NDVI value for this pixel is 0.24 (image 59) which occurred during late spring in November 2002. The maximum NDVI value for this pixel is 0.67 (image 79) which occurred during early spring in September 2003. The NDVI values in the third pixel fluctuate more than the other soil pixels. The NDVI values of the first two soil pixels have a larger range of 0.17 to 0.92 and 0.18 to 0.95, but the third soil pixel has a NDVI range from 0.24 to 0.67. The smaller NDVI range and the rapid fluctuations in NDVI values indicate this pixel is partially vegetated throughout the year. The minimum NDVI values for all three soil pixels occur in November 2004, November 2003 and November 2002 during late spring when vegetation experiences little growth. These results indicate that the reflectance of soil pixels vary annually and seasonally. Soil reflectance is affected by the amount of soil moisture and soil texture (Farrar *et al.* 1994). Surface roughness, the amount of organic matter and iron oxide will also affect soil reflectance (Lillesand and Keifer 1994). These factors could explain the erratic patterns in the spectral signature (i.e. noise in the data). Out of the three soil pixels the second pixel had the most productive crop years out of the three, but in terms of overall productivity throughout time the third soil pixel has the highest productivity out of the three soil pixels due to a higher occurrence of greenness (NDVI) over time. The minimum and maximum NDVI values for the soil pixels are listed in Table 3.

3.1.2 Spectral signatures of vegetation pixels

The spectral signatures for three vegetation pixels are shown below in Figure 10.

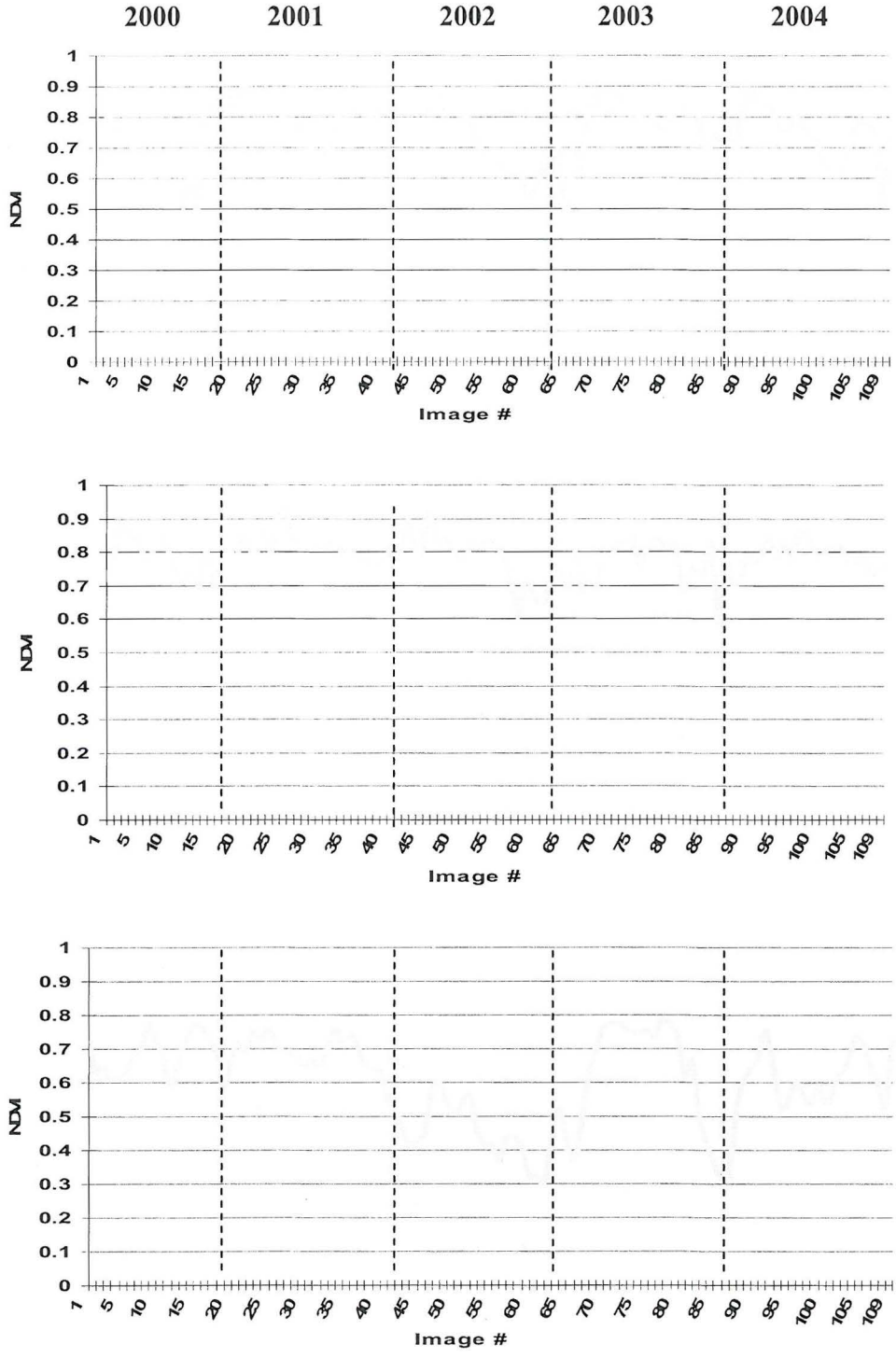

Figure 10. NDVI values of three pixels assumed to contain vegetation

Vegetation pixels display different spectral signatures than soil pixels. In the vegetation pixel analysis the maximum NDVI values indicate periods of intense greenness or higher NDVI values overall. The minimum NDVI values or the troughs generally indicate a lack of water or soil moisture at a particular point in time. By analysing the troughs, dry periods can be noted. It is interesting to note the dry periods since the high rain variability will affect the rates of vegetation growth causing numerous peaks.

In the first vegetation pixel there are three evident troughs. The first trough occurred in November 2000 (image 18) with minimum NDVI value of 0.51. This trough occurred during late spring. The second trough occurred in January 2003 (image 64) with a minimum NDVI value of 0.48. This trough occurred during the driest period out of the four years in the middle of summer. The third trough occurs in December 2004 (image 107) with a minimum NDVI value of 0.51. The overall minimum NDVI value for this pixel is 0.48 (image 64) and the maximum NDVI value is 0.91 (image 20) which occurred in February 2001.

In the second vegetation pixel there are three troughs in the spectral signature. The first one occurs in December 2000 (image 15) with a NDVI value of 0.68. The second trough occurs in November 2002 (image 60) with a NDVI value of 0.65. The third trough occurs during December 2003 (image 85) with a NDVI value of 0.57. All of the minimum NDVI values for this pixel occur during late spring. The NDVI values for this pixel have a minimum of 0.57 (image 85) and a maximum of 0.94 (image 25). The maximum NDVI value occurred in May 2001. The second vegetation pixel has the smallest NDVI range when compared with the other two vegetation pixels. This indicates that this pixel is more productive than the other vegetation pixels due to the occurrence of higher NDVI values through time. The density of the canopy in this pixel is higher than the other pixels increasing the green reflectance picked up by the satellite (Figure 10).

There are also three troughs evident in the third vegetation pixel. The first trough occurred in February 2002 (image 43) with a minimum NDVI value of 0.42. The second trough occurred in December 2002 (image 61) with a minimum NDVI value of 0.3. The third trough has an NDVI value of 0.3 and occurs during December 2003 (image 85). The NDVI values for this pixel have a minimum NDVI value of 0.3 and a maximum NDVI value of 0.79 (image 77). The third vegetation pixel has a different pattern than the first two vegetation pixels and has a larger range of NDVI

values than the other vegetation pixels, suggesting that this pixel is likely to be in an area with low soil moisture. The third pixel does not experience a major decrease in NDVI until 2002 when soil conditions would have been dry from the drought. All three vegetation pixels show decreases during 2002. The minimum and maximum NDVI values for vegetation pixels are listed in Table 3.

Table 3. NDVI ranges for soil and vegetation pixels.

Pixel	**Minimum NDVI**	**Maximum NDVI**	**Difference**
Soil1	0.17	0.92	0.75
Soil2	0.18	0.94	0.76
Soil3	0.24	0.67	0.43
Veg1	0.48	0.91	0.43
Veg2	0.57	0.94	0.37
Veg3	0.30	0.79	0.49

The first two soil pixels have a high range of NDVI values while the third soil pixel falls within the ranges of the three vegetation pixels. The first two soil pixels have ranges of 0.75 and 0.76 while the third soil pixel has a range of 0.43. Soil pixels have higher ranges of NDVI values than pixels containing vegetation. The three vegetation pixels have ranges of 0.42, 0.36 and 0.49. When compared with the vegetation pixels, the soil pixels have the highest range of NDVI values. The third soil pixel contains more vegetation throughout the year than the first two soil pixels and has a lower maximum NDVI value then the vegetation pixels suggesting there is a larger proportion of soil than vegetation on this pixel.

3.1.3 Spectral signatures of water pixels

The spectral signatures for three water pixels are shown below in Figure 11.

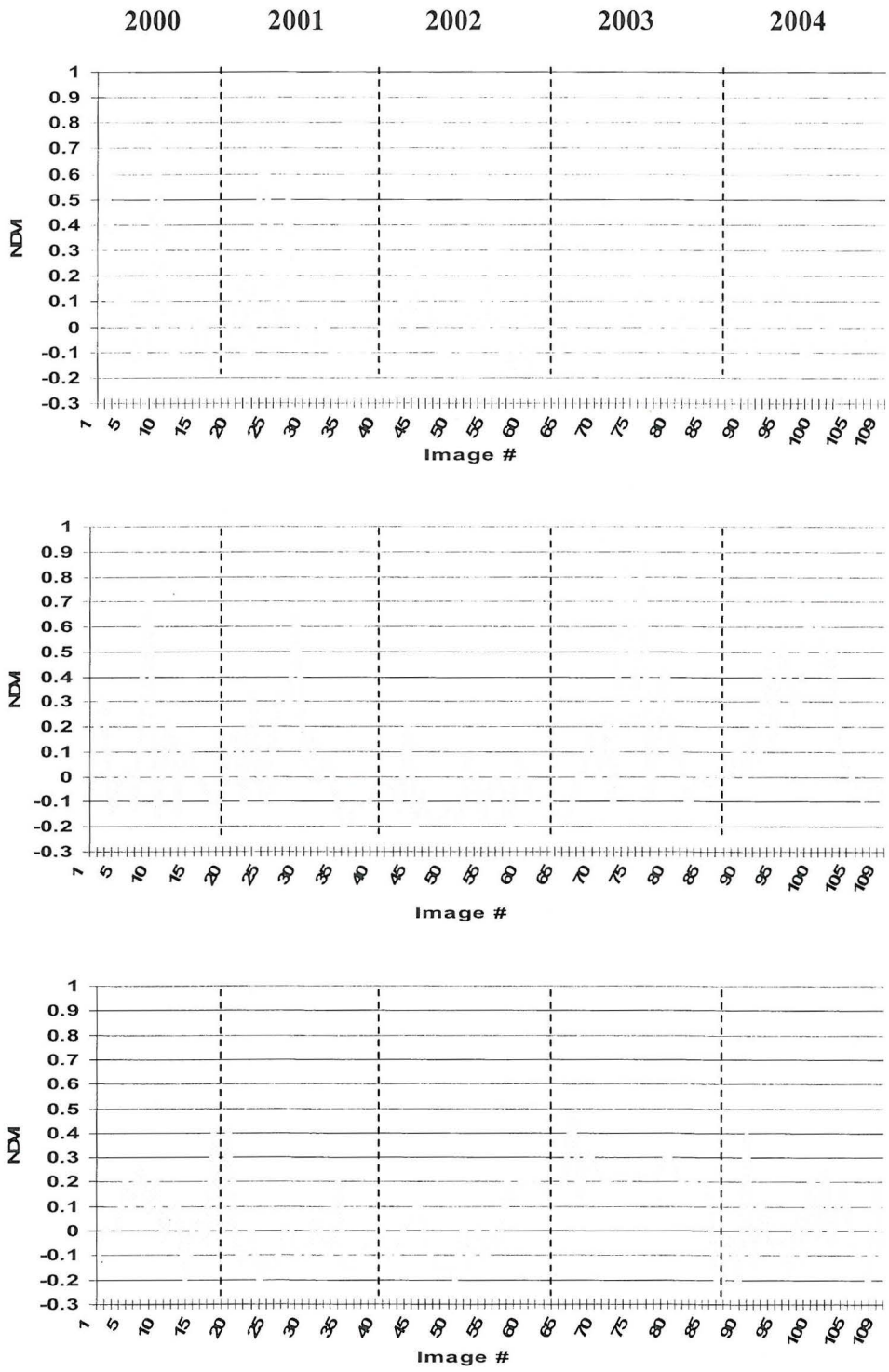

Figure 11. MODIS NDVI values of three pixels assumed to contain water.

The water pixels have more inconsistent patterns in their spectral signatures than the soil and vegetation pixels. The water pixels experience rapid changes in NDVI compared to the soil and vegetation pixels. The NDVI value ranges are much higher than the soil and vegetation pixels. The first water pixel ranges from -0.18 to 0.79. The second water pixel ranges from -0.2 to 0.86 and the third water pixel ranges from -0.2 to 0.49. This is due not only to the dark colour of the water surface, but also the high reflectance off the water surface. Water is in constant motion at the surface so the reflectance will have high variance and change rapidly whereas vegetation and soil pixels are stationary and have less variance. Some factors affecting water reflectance include interactions at the water surface, suspended materials which usually have a higher reflectance and the bottom of a water body (Lillesand and Kiefer 1994). The first and second water pixels have similar spectral signatures (Figure 11) with sharp peaks and rapid changes in NDVI values. The third pixel however has a smaller pixel value range and contains smaller peaks, but still displays a rapid change in NDVI value over time. The third water pixel has an NDVI value range of -0.2 to 0.49. The smaller range could be explained by the depth of the water. The third pixel is most likely a farm dam or perhaps a temporary water body due to the wetting and drying pattern in the spectral signature. The first and second pixels are likely to be permanent, deeper water bodies due to the constant variation of NDVI values. The high peaks of NDVI values in the water pixels (pixel 1 = 0.8, pixel 2 = 0.86 and pixel 3 = 0.49) indicate vegetation growth. It would be interesting to check the high peaks of NDVI to see if MODIS data can pick up blue-green algal blooms in water. The water pixels were mainly used as a comparative analysis in pixel NDVI values and to see how these values vary and compare with the soil and vegetation pixels.

3.1.4 Monthly average NDVI

The NDVI is strongly correlated with the fPAR absorbed by vegetation (Asrar *et al.* 1984; Huemmrich and Goward 1997); therefore, estimates of fPAR can be derived from MODIS NDVI data. Hence, the amount of water used to acquire carbon (GPP) can be used estimate the transpiration flux of the vegetation. Soil pixels tend to have a larger range of NDVI values due to the higher fluctuations of greenness experienced throughout the growing season. Crops grow over a period of three months and are then harvested. This changes the spectral signature dramatically from higher NDVI values to lower NDVI values (bright green vegetation to brown bare soils). The vegetation pixels have a NDVI range which is significantly smaller than the soil pixels. Pixels that

contain vegetation stay greener for longer, resulting in a decrease in the variance of NDVI values. NDVI values decrease during winter months due to decreased light and water availability. NDVI values start to increase throughout spring due to increased water availability unless there are drought conditions (i.e. 2002). 2002 was the driest year out of the five and coincides with low NDVI values. The low NDVI values were then carried over into the beginning of 2003.

NDVI estimates were averaged in monthly intervals to identify trends in NDVI over seasons in the vegetation pixels. Then the MODIS images were averaged on a monthly basis for years 2000 to 2004. The monthly NDVI values for the three vegetation pixels are displayed in Figure 12 with each line representing one year (2001-2004).

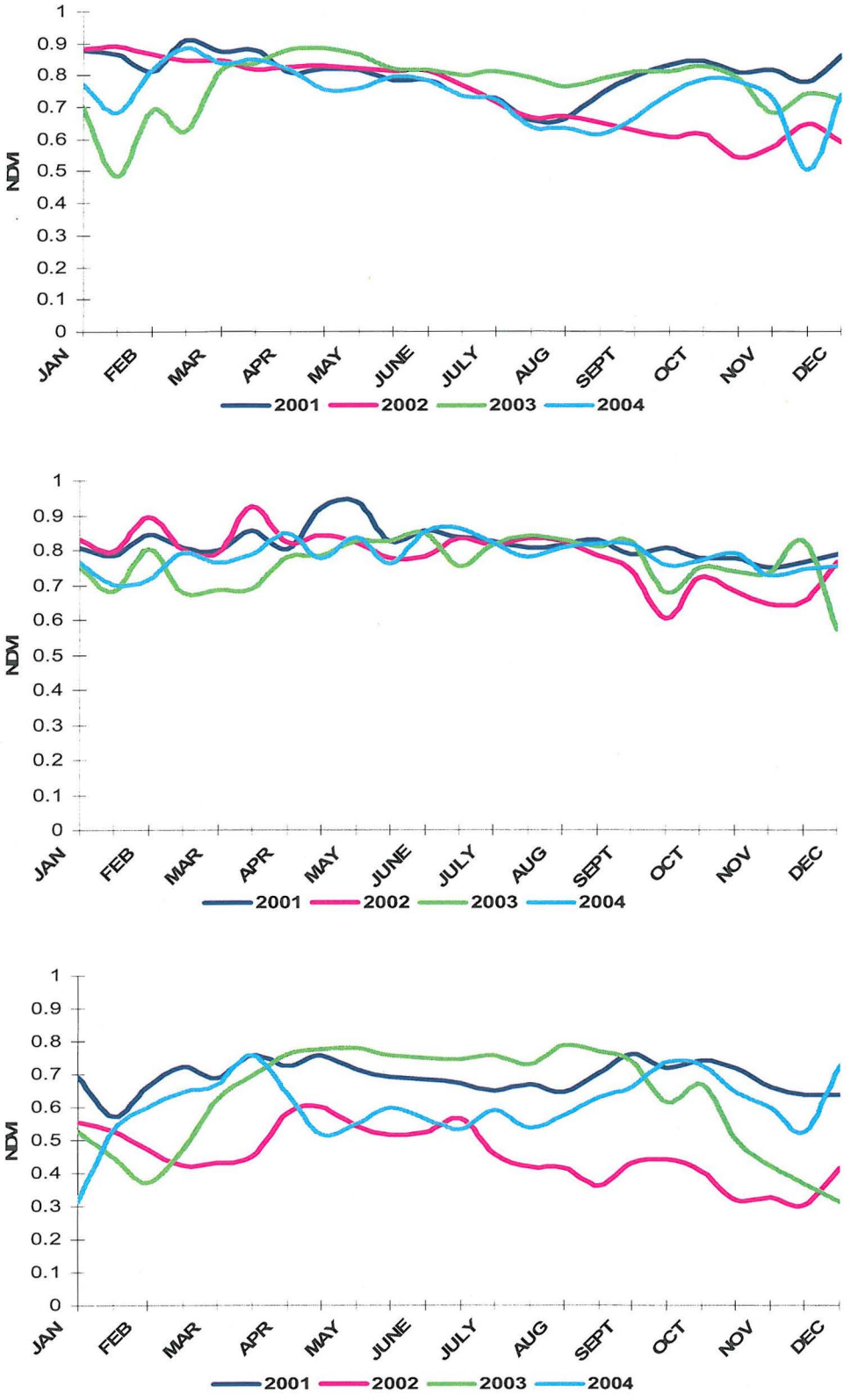

Figure 12. Monthly average for MODIS NDVI data for vegetation pixels (2001-2004).

NDVI data for the year 2000 was left out due to missing monthly data for that year from January to the beginning of April. The monthly NDVI in the first pixel decreases slightly during the winter months due to lower temperatures and reduced soil moisture. In 2002, the first vegetation pixel displays the lowest monthly NDVI value in December 2002. This carries over into 2003 with January 2003 having the lowest NDVI value over the four years. The year 2002 was the driest year out of the four years. This resulted in lower NDVI values due to the lack of soil water for plant uptake. During the winter months the NDVI values for the second pixel did not show a distinct downward trend in NDVI. The first and second pixels display the lowest monthly NDVI values in January 2003. The second vegetation pixel had the least variation of NDVI values. This suggests that this pixel is located on a site where water availability is not limiting. The second vegetation pixel displays stable NDVI values in the winter months while the third vegetation pixel shows increased inter-annual variability. The third vegetation pixel had the highest spread of values suggesting that this pixel is partially vegetated or is located in an area where soil water is limited. Partially vegetated pixels will vary in NDVI values more than pixels that are covered in a higher percentage of green vegetation. Partially vegetated pixels will vary in NDVI because they contain a mixture of land cover types. These pixels are reflecting a mixture of vegetation, soil and perhaps water causing increased distortion in the spectral signature of the pixel. Whereas a pixel containing mostly vegetation will not vary as much as a pixel with mixed coverage.

3.2 Transpiration fluxes of croplands and non croplands

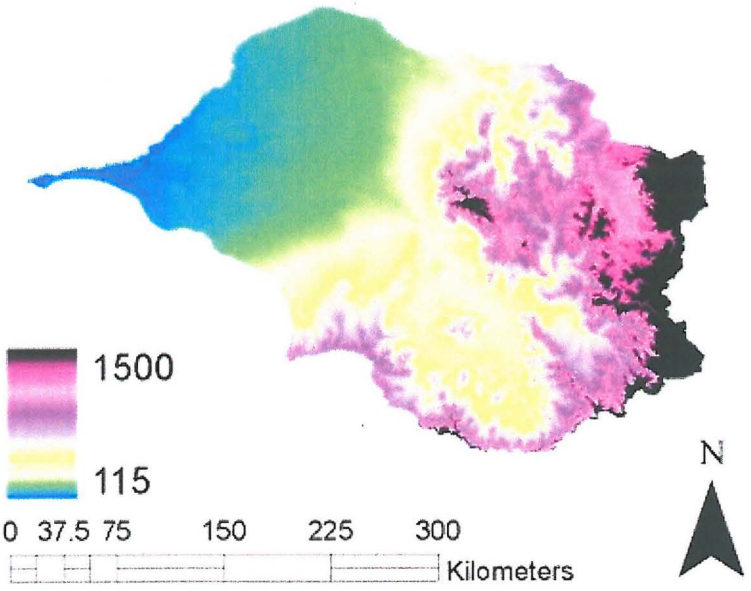

Figure 13. Digital Elevation Model of the Gwydir and Namoi catchments.

3.2.1 Catchment level estimates of fPAR

Pixels containing cropland were extracted by calculating the mean, variance, standard deviation and COV of the monthly fPAR grids derived from NDVI data in order to investigate the changes in transpiration fluxes between croplands and non croplands. As noted above, studies have found that NDVI and fPAR are correlated in a near linear relationship (Asrar *et al.* 1984; Asrar *et al.* 1992; Sellers 1985). Since fPAR is correlated with NDVI, the monthly fPAR grids were used to extract the spectral signature of croplands. The mean and variance were calculated as inputs to evaluate the standard deviation. Figure 14 shows the resulting maps of the mean, standard deviation and COV calculations.

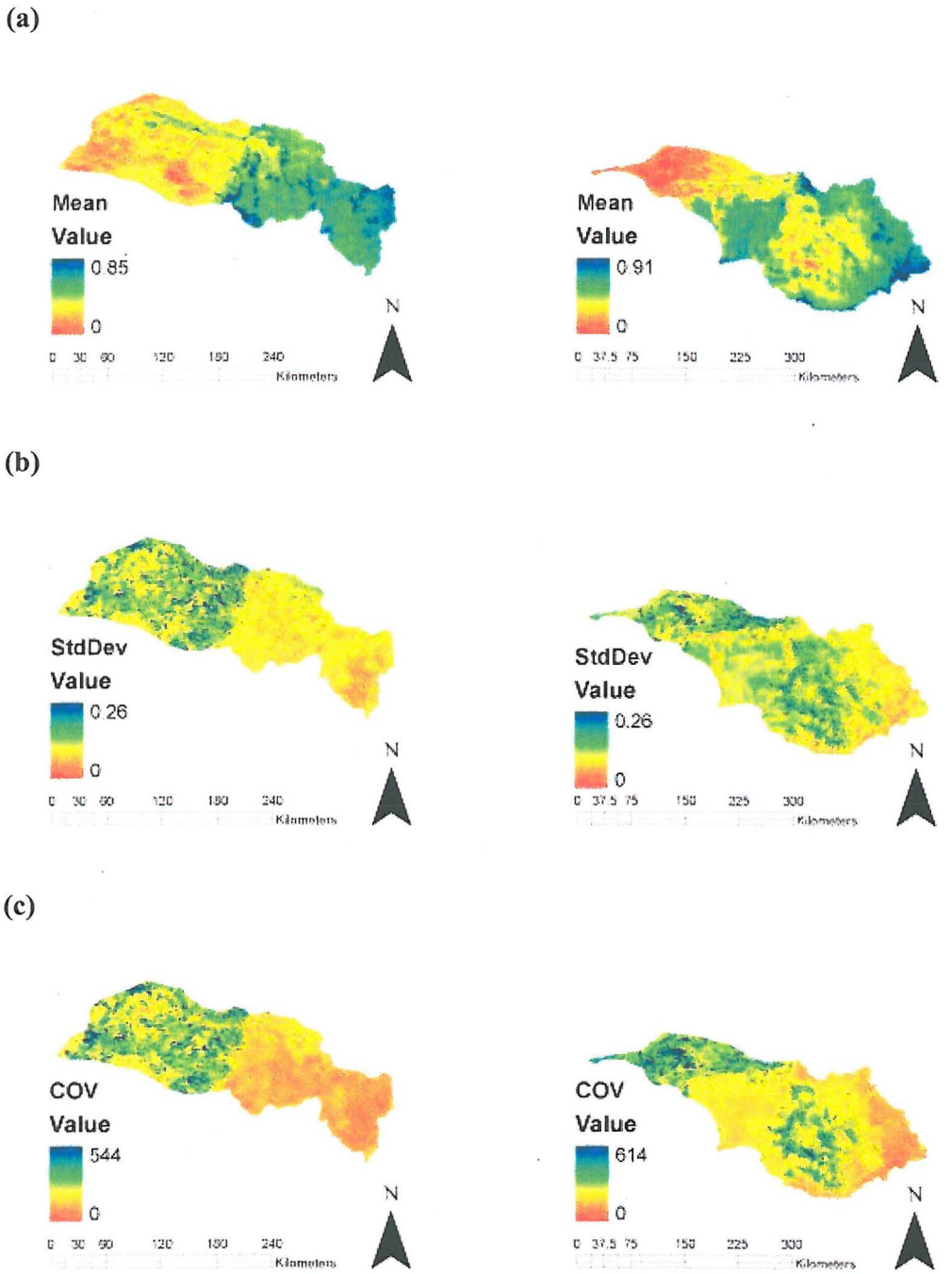

Figure 14. The (a) mean, (b) standard deviation and (c) COV of fPAR in the Gwydir and Namoi catchments.

The mean fPAR across all four years of data from 2001 to 2004 was used. The minimum mean fPAR value in the Gwydir catchment was 0 and the maximum value was 0.85. The minimum mean fPAR value in the Namoi catchment was 0 and the maximum mean value was 0.91. Since non croplands are utilising fPAR for photosynthesis throughout year they have higher mean fPAR values while croplands are utilising fPAR at certain times during the year therefore they have low mean fPAR values. This is evident when comparing Figures 9 and 10. Croplands are located in the western regions of the Gwydir and Namoi catchments as well as the central portion of the Namoi. The Namoi catchment has a higher mean fPAR than the Gwydir catchment because the Namoi catchment has more non cropland area than the Gwydir catchment.

Obtaining the standard deviation of the fPAR data provides a measure of the variation in the data. The standard deviation is higher in the western regions of both catchments and in parts of the central Namoi catchment, indicating croplands in these regions. Both catchments have a minimum standard deviation of 0 and a maximum standard deviation of 0.26. Croplands become evident in the standard deviation maps and are enhanced in the COV maps.

The COV was calculated over the four years of data to further enhance the variation between the cropland and non cropland pixels. As a result the cropland and non cropland pixels can be distinguished. The COV is the standard deviation conveyed as a percentage of the mean (Sokal and Rohlf 1995). The COV calculation widens the gap between the fPAR values of pixels containing croplands and non croplands. Compare Figures 14b and 14c. The range of the COV values in the Namoi catchment was 0 to 614 and 0 and 544 in the Gwydir catchment. Vegetation canopies growing on soils deprived of nutrients will have long-lived leaves and therefore show little variation in fPAR over time while canopies growing on nutrient rich soils will show large variation in fPAR over time (Berry and Roderick 2002b). The COV values vary significantly between cropland and non cropland pixels due to the fluctuation in greenness values in croplands throughout the year. Croplands have a higher COV than non croplands because they are utilising fPAR for a smaller period of time during the year. Therefore shorter growing seasons have larger variations in COV values of fPAR due to the change from green vegetation to bare soil in the spectral signature over time. The non cropland pixels have lower COV values because the greenness values are similar throughout the year as long as extremely dry periods are avoided. Non croplands are using fPAR all year and therefore have smaller variations in COV values

of fPAR. Low values of COV occurred on high elevations in both catchments, indicating a high density of evergreen vegetation.

3.2.2 Transpiration fluxes of individual pixels

Eight pixels were chosen from the COV grids to compare the differences in transpiration fluxes between cropland (pixels *a*, *b*, *c* and *d*) and non cropland (*e*, *f*, *g* and *h*). The spatial arrangement of pixels in the COV grids assisted in the identification of cropland and non cropland pixels. Croplands were clustered in rectangular plots while non cropland pixels were scattered across the landscape. For every pixel assessed, there were five major peaks in transpiration fluxes, one peak for each year from 2000-2004. Monthly estimates of transpiration fluxes for cropland and non cropland pixels are displayed in Figure 16. There are smaller peaks that occur within the large peaks of transpiration fluxes indicating periods of vegetation growth. For cropland pixels, the major peaks occurred mainly in the beginning of spring in September, but peaks also occurred in late winter during August, mid-spring in October and in the beginning of summer in December. The smaller peaks in transpiration fluxes occurred in 2000 with two peaks in pixels *b*, *c* and *d*. Pixel *a* is the most productive out of the four cropland pixels. The transpiration values for pixel *a* are as follows: year 2000: 72kg m^{-2} $year^{-1}$, year 2001:70kg m^{-2} $year^{-1}$, year 2002: 38kg m^{-2} $year^{-1}$, year 2003: 67kg m^{-2} $year^{-1}$ and year 2004: 68kg m^{-2} $year^{-1}$. The years 2000 and 2002 experienced higher variation in transpiration with 2000 being the wettest year and 2002 being the driest year. In 2001, 2003 and 2004 all crop pixels had similar transpiration fluxes. Figure 15 displays the annual transpiration fluxes for cropland pixel *b* and non cropland pixel *e*. Pixels containing non cropland peaked at different times throughout spring and summer and in some cases for longer periods then pixels containing croplands. This is evident when comparing Figures 16a and 16b. These peaks occurred in January, March, April, September, October, November and December. For years 2001 through 2004 the cropland pixels had one peak in transpiration for each year. See Figure 16 a. All four non cropland pixels had one peak of transpiration in 2002. These peaks occurred in December for pixels *e* and *f*, October for pixel *g* and March for pixel *f*. Out of the four non cropland pixels, pixel *g* is the most productive with the highest transpiration flux throughout time. The minimum transpiration value for pixel *g* is 45kg m^{-2} $month^{-1}$ which occurred during October 2002. The maximum transpiration value for pixel *g* is 75kg m^{-2} $month^{-1}$ which occurred during December 2000. The non cropland pixels have a longer active growing season than the cropland pixels.

(a)

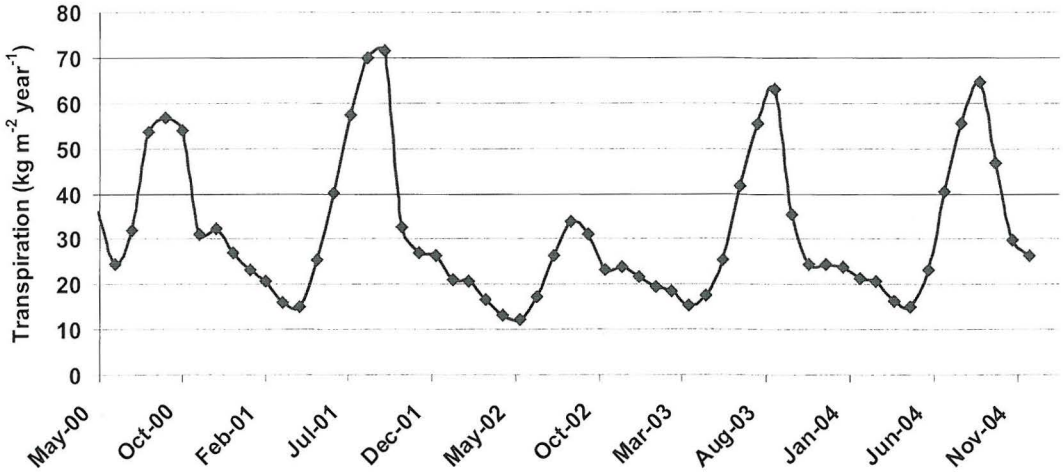

(b)

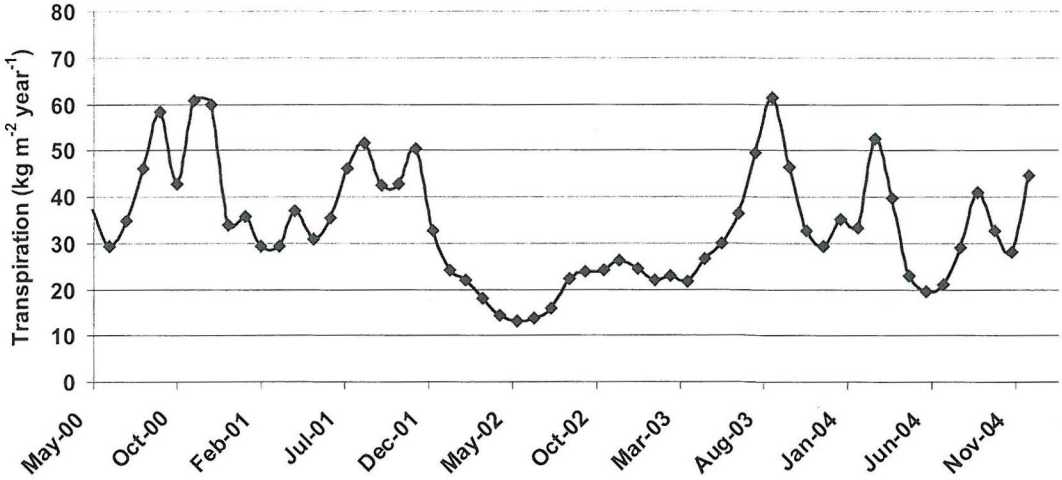

Figure 15. Annual transpiration (kg m-2yr-1) for (a) cropland pixel b and (b) non cropland pixel *e*.

The lowest values of transpiration occurred during the year 2002 for all pixels. Five out of the eight pixels had the highest values of transpiration that occurred during the year 2000. Two non cropland pixels had the highest transpiration during 2003 and one of the cropland pixels had the highest transpiration during 2001. The lowest transpiration value occurred in December 2002 in the cropland pixel *d* with a value of 21kg m^{-2} $month^{-1}$. The highest transpiration value occurred in December 2000 in the non cropland pixel *f* with a transpiration value of 80kg m^{-2} $month^{-1}$. The cropland pixels show the highest variation in transpiration fluxes throughout time. The largest

difference in transpiration fluxes for cropland pixels is 53kg m^{-2} $month^{-1}$ and the largest value for non cropland pixels is 43kg m^{-2} $month^{-1}$. Pixel *g* seems to be transpiring the most over time with the smallest fluctuation in transpiration fluxes. All four non cropland pixels displayed different amounts and patterns of transpiration from 2000 to 2004. Crops utilise fPAR for a smaller amount of time over the course of one year. As a result, crops do not transpire as much as the vegetation present on non croplands. Non cropland pixels utilise fPAR throughout the year and thus have higher transpiration fluxes than crops.

3.2.3 Annual transpiration fluxes in the Gwydir and Namoi catchments

In the Gwydir and Namoi catchments the majority of cropland pixels lie in the western region of the catchment in the flat, fertile, floodplain areas. The Namoi catchment also has a concentration of cropland pixels near major towns in the central part of the catchment particularly near Gunnedah (Figure 18). Figure 16 shows the comparison between the annual transpiration fluxes for the cropland and non cropland pixels. The non cropland pixels have more variation in transpiration fluxes compared to the cropland pixels. Croplands are responding to a regular water supply via irrigation whereas the non croplands are responding to natural rainfall amounts. Croplands are planted at the same time whereas non croplands are relying on their own seed store.

Some non cropland pixels can be observed following watercourses such as the Gwydir and Namoi Rivers from the central catchment area heading west. This is evident in Figure 17 for both catchments on the 2001 maps. It is also apparent in the western Gwydir catchment in the Gwydir wetlands. Plants in this area are transpiring more water due to the increased availability of water from the wetlands. Pixels containing non croplands tend to transpire more water due to higher water holding capacity and leaf surface area exhibiting characteristics similar to forests. This trend is evident in the Gwydir and Namoi catchments. The non cropland pixels display higher transpiration fluxes than the cropland pixels. Peaks of transpiration indicate when plants are releasing the most water into the atmosphere. Since GPP is directly linked with transpiration this suggests that the highest transpiration fluxes occur during peak productivity. Non cropland pixels have rounded peaks in transpiration than pixels containing croplands (Figure 16). This supports the idea that evergreen vegetation stays greener longer than croplands due to extended periods of transpiration. When crops reach the greenest point they are harvested shortly after. The spectral signature for the

cropland pixel changes from a vegetated NDVI value (~0.4-0.7) to a soil NDVI value (~0-0.17). The higher number of small transpiration flux peaks that occurred during a given year suggest that year had more wet events compared to other years. These peaks are likely to coincide with available soil water. The lowest transpiration fluxes occurred during 2002. In this case, 2002 was the driest year with one major peak for all eight pixels over cropland and non cropland. This corresponds with one of the worst droughts on record and the effects on transpiration are evident. The lack of rain during 2002 limited soil water availability, causing plants to decrease the size of their stomata in order to conserve water. Rainfall gauges in the Gwydir and Namoi reported noticeable decreases in yearly rainfall totals. For example, in the Namoi the Barraba post office (054003) reported 686mm for 2001 and 330mm for 2002 and the Wee Waa (George St.) (053044) rain gauge reported 627mm for 2001 and 268mm for 2002. Drought conditions would have caused the stomates to close for a longer period compared to wetter years. Years 2000, 2001, 2003 and 2004 all experienced minor peaks among the large peaks of transpiration.

Areas of non croplands had higher transpiration fluxes than areas with croplands. The Namoi catchment has more non cropland area than the Gwydir catchment (21047km^2). The Namoi catchment has 5244km^2 of croplands and 36736km^2 of non croplands. The Gwydir catchment has more cropland area than the Namoi with 5529km^2 and 21047km^2 of non croplands (Table 5). Since the Namoi has more non croplands area, it also has higher annual transpiration fluxes than the Gwydir catchment. In 2001, the annual transpiration flux for non croplands in the Namoi catchment was 3.0E8 kg m^{-2}yr^{-1} compared to 1.69 kg m^{-2}yr^{-1} in the Gwydir catchment. Since the Gwydir has more cropland area than the Namoi, the Gwydir catchment has higher annual cropland transpiration than the Namoi for years 2001, 2002 and 2004 (Table 4). In 2003, the Namoi catchment had higher annual cropland transpiration flux than the Gwydir catchment with 2.65E7 kg m^{-2}yr^{-1} in the Namoi and 2.56 kg m^{-2}yr^{-1}. Due to the drought in 2002, farmers were likely to be using more water in both catchments in 2003 to ensure crop growth to cover financial losses from the previous year. Interestingly, the transpiration fluxes increased 12% from 2002-2003 in the Namoi catchment cropland pixels. In the Gwydir catchment the transpiration fluxes increased by 8% from 2002-2003 in the cropland pixels. This shows that the water use on croplands in the Gwydir and Namoi catchments increased after the drought. Water use increased more in the Namoi catchment even though the Namoi catchment has a smaller area of croplands compared to the Gwydir catchment. This is most likely due to

the large tracts of agricultural land dedicated to cotton crops. In 2001 and 2004, annual estimates of transpiration fluxes for vegetation pixels account for 84% of the transpiration in the Gwydir catchment while croplands contribute 16%. In 2002 and 2003, the non cropland pixels contributed 85% and the croplands were responsible for 15% of annual transpiration. In 2001, 2003 and 2004, annual estimates of transpiration fluxes account for 91% transpiration in the Namoi catchment while croplands contribute 9%. In 2002, the non cropland pixels contributed 92% while the croplands contributed 8% of transpiration.

Table 4. Annual transpiration fluxes (kg m-2yr-1) in the Gwydir and Namoi catchments.

	2001	2002	2003	2004
Gwydir	2.01E8	1.52E8	1.74E8	1.95E8
Namoi	3.31E8	2.5E8	2.99E8	3.25E8

Table 5. Cropland vs. non-cropland transpiration fluxes (kg m-2yr-1) in the Gwydir and Namoi catchments.

	2001	2002	2003	2004
G_crop	3.26E7	2.21E7	2.56E7	3.2E7
G_non_crop	1.69E8	1.3E8	1.48E8	1.63E8
N_crop	3.06E7	2.07E7	2.65E7	3.03E7
N_non_crop	3.0E8	2.3E8	2.73E8	2.95E8

Figure 17 displays the annual transpiration trends over the Gwydir and Namoi catchments. These areas are classified as non cropland pixels. According to Carnahan's AUSLIG vegetation dataset they contain eucalypt dominated forests with 30-70% cover. 2002 had the lowest overall annual transpiration fluxes while 2001 had the highest overall transpiration fluxes throughout the year. The majority of water used in agriculture in these catchments is mainly for irrigation. In the Gwydir catchment the Gwydir wetlands provide an additional water supply for irrigation farming. The cropland pixels experienced the most variation in transpiration values during 2000 and 2001. According to the annual transpiration rates in Figure 16, the non cropland pixels have the highest transpiration fluxes for years 2000 and 2001 indicating that these were particularly wet years. After the 2002-2003 drought transpiration fluxes increased over time during the vegetative recovery period.

3.31E8kg $m^{-2}yr^{-1}$ and 2.01E8kg $m^{-2}yr^{-1}$ for the Gwydir. In comparison, the annual transpiration flux across the whole catchment for the Namoi in 2002 was

2.5E8kg $m^{-2}yr^{-1}$ and 1.52E8kg $m^{-2}yr^{-1}$ for the Gwydir. The difference in transpiration fluxes in the Gwydir and Namoi catchments from the wettest year in 2001 to the driest year in 2002 is 1.29E8kg $m^{-2}yr^{-1}$; which is ~25% decrease in transpiration over both catchments in one year (Table 4). As a result, 2002 was a devastating year for crop growth.

Changes in transpiration fluxes are also affected in part by the topographical position of the plant in the catchment. Barrett *et al.* (1996) found that eucalypt forests and rainforests on the southerly aspect had similar transpiration rates throughout the year. Since precipitation increases with altitude (assuming moisture-bearing clouds are present) it would be expected that transpiration fluxes would also increase. When comparing the DEM (Figure 13) and the transpiration rates across the Gwydir and Namoi catchments (Figure 17) a similar pattern of increased transpiration fluxes on southerly aspects emerges. In Figure 17 there are also prominent increases in transpiration fluxes in areas of high elevation.

(a)

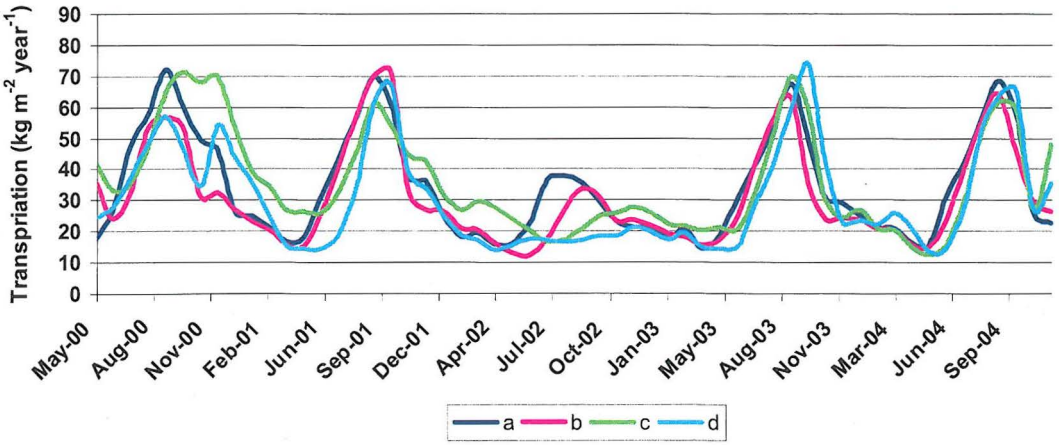

(b)

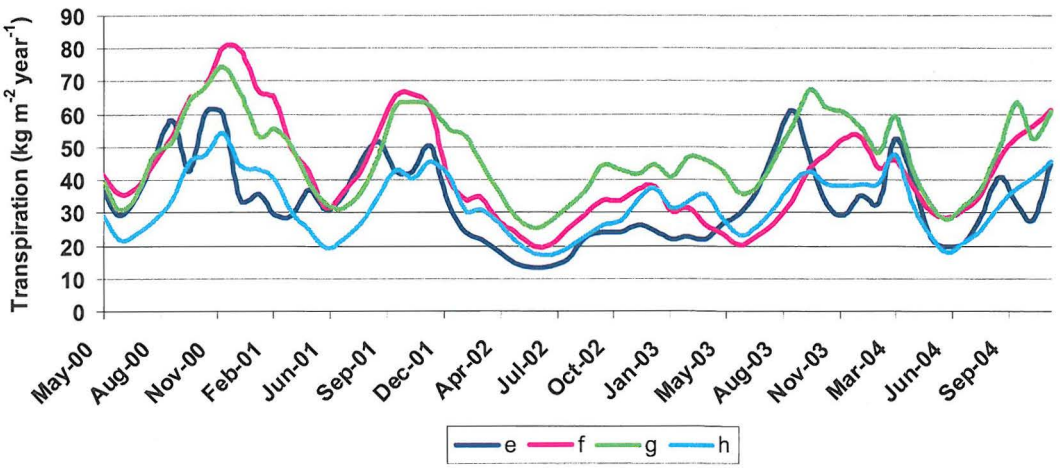

Figure 16. Annual transpiration (kg m-2yr-1) for (a) cropland pixels and (b) non cropland pixels from May 2000 to December 2004 (Gwydir and Namoi catchments).

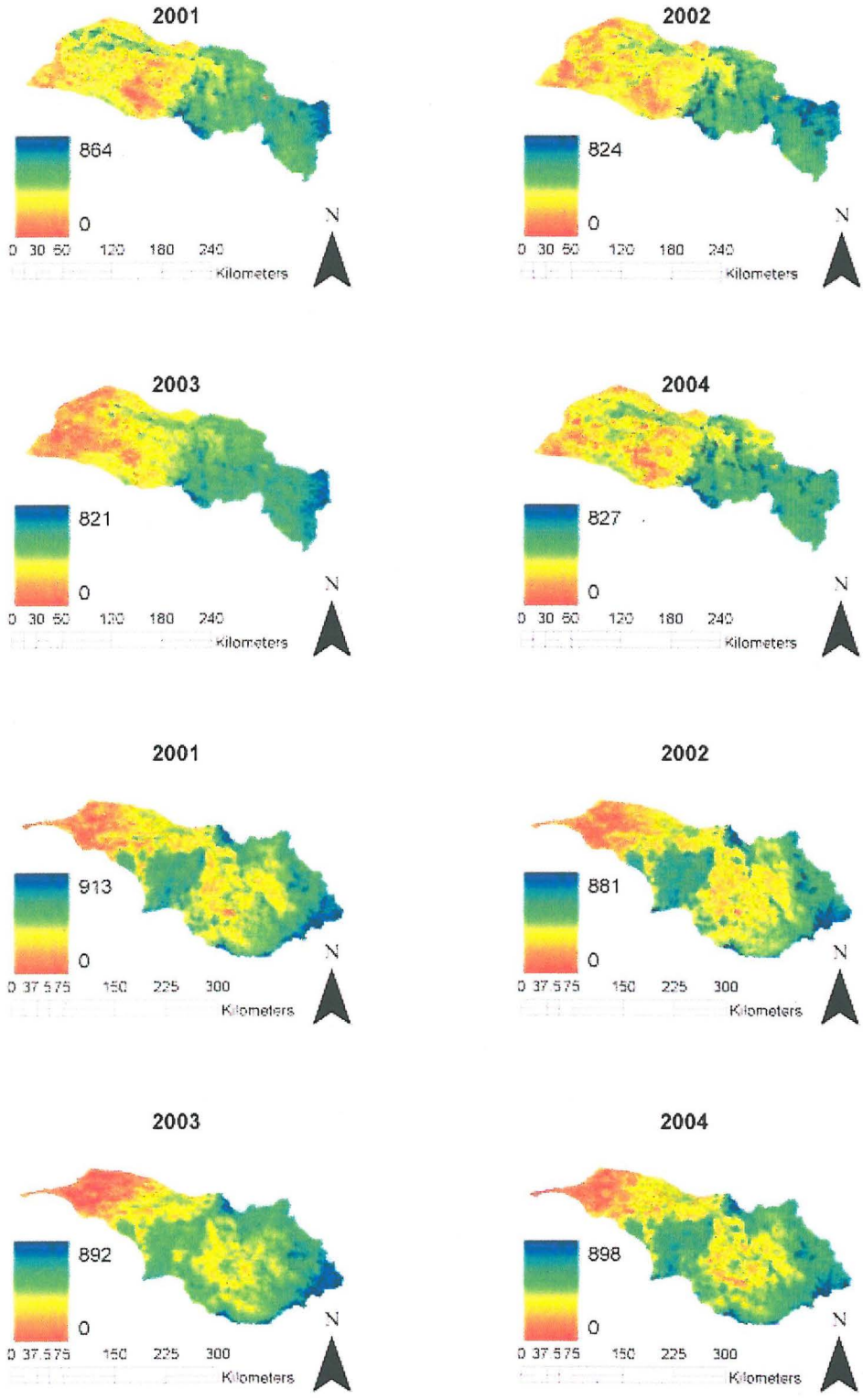

Figure 17. Annual transpiration (kg m-2yr-1) across the Gwydir and Namoi catchments for years 2001-2004.

3.3 Comparison of vegetation datasets

The Carnahan's AUSLIG vegetation dataset represents the vegetation types in Australia present in 1988. This data has a coarse scale resolution of 5km. The MODIS data is more recent land coverage (April 2000-December 2004) data at a high resolution of 250m. These datasets were compared in order to check the accuracy of the descriptive statistics calculations performed in IDRISI to separate cropland from non cropland pixels in the Gwydir and Namoi catchments. Some very interesting patterns emerged when the grids were overlayed. Figure 18 displays the croplands extracted from the fPAR grids derived from the MODIS NDVI data and the Carnahan's AUSLIG vegetation dataset. The polygons outlining the croplands are from the Carnahan's AUSLIG vegetation dataset. When these datasets were compared the croplands and non croplands displayed similar trends in land use coverage. In the MODIS data, individual croplands are apparent rectangular shapes spread out across the landscape in clusters. In the coarse resolution dataset the vegetation is represented by rough polygons of where particular vegetation communities occur.

According to Carnahan's AUSLIG vegetation dataset, there are three broad types of vegetation that occur in the Namoi and Gwydir catchments, these are classified as eucalypt, conifer and grasses. Eucalyptus trees have extensive horizontal root systems (Eldridge and Freudenberger 2005). In water-limited environments, many woody evergreen plants have extensive root systems and also store water in their leaves for later use (Berry *et al.* 2005). Eucalypts can tap into water 20m below the surface and hence transpire water from greater depths than crops and grasses (Stirzaker *et al.* 1999). Extensive root systems allow for an increased root surface area in which trees can absorb and transport large amounts of water. Shallow rooted crops tend to absorb and transport less water than eucalypts. Differences in rooting depth affect transpiration fluxes (Nepstad *et al.* 1994). Since trees have a larger water capacity than herbaceous plants; we can assume that transpiration rates over forested canopies are higher than grasslands or croplands. Eucalypts have evolved deep root systems able to extract water deep within soil profile; replacement of native trees with plants that have shallow root systems alters hydrology by altering water table levels which in some cases can lead to dryland salinity.

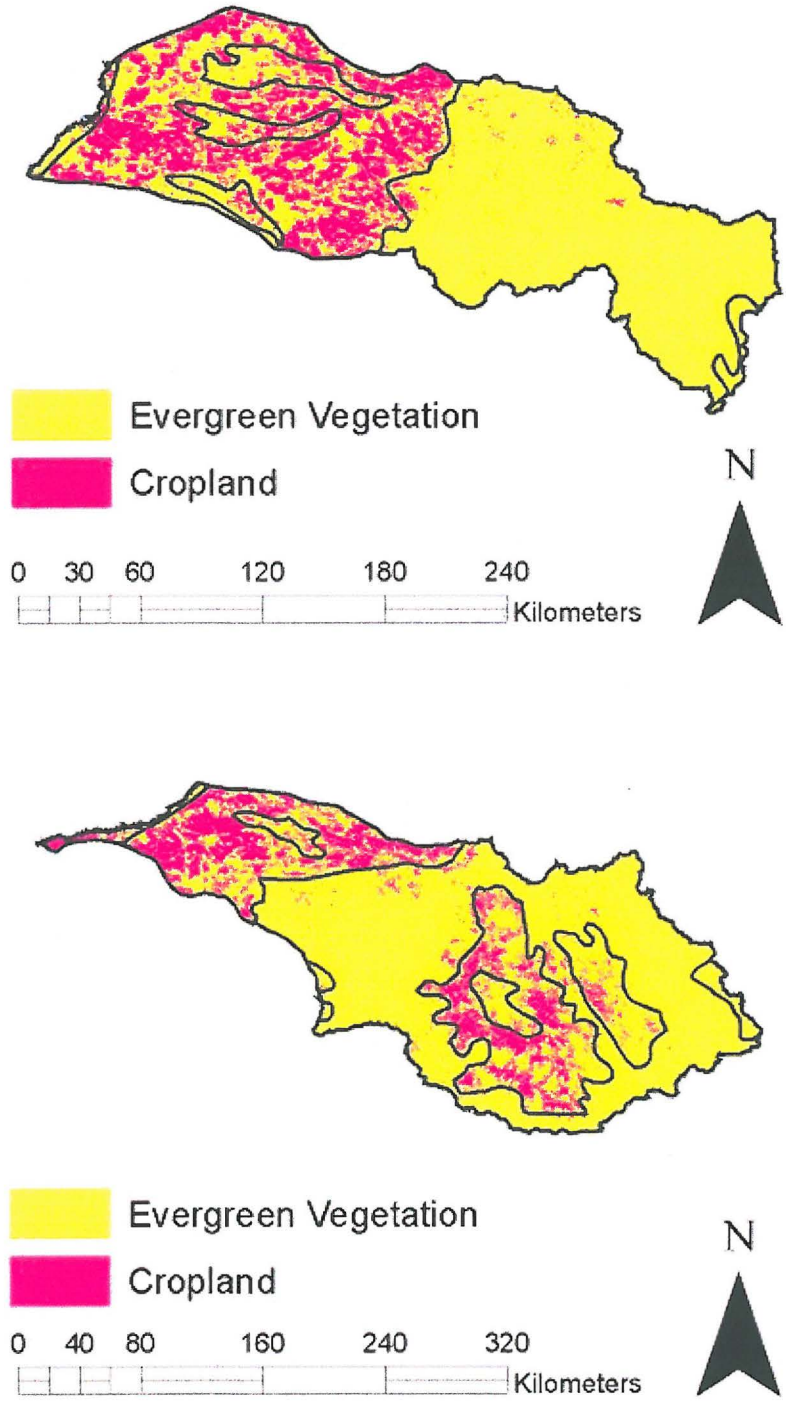

Figure 18. Comparison of Carnahan's vegetation dataset boundaries (bold outline) and croplands extracted from MODIS data (pink areas).

When comparing the Carnahan's AUSLIG vegetation dataset with the croplands extracted from the MODIS data it is apparent that some of the areas that were classified as evergreen vegetation in 1988 have been converted to agricultural land. This is shown in the comparison maps (Figure 18) where the croplands are apparent in the polygons classified as evergreen vegetation. Some croplands extend outside of the polygons. This is increasingly noticeable in the Gwydir catchment particularly in the Gwydir wetlands. Croplands are encroaching on the wetlands. One of the greatest impacts since European settlement is the removal of vegetation in wet environments (Berry and Roderick 2002a). Large scale vegetation clearance or conversion could change local climate regimes (Fu *et al.* 2005) through alterations in the hydrologic cycle. The removal of forest can also influence the surface roughness affecting transpiration rates. The replacement of trees with shallow rooted plants can cause water tables to rise and in some cases causing salinity problems. The conversion of the Gwydir wetlands is likely to continue into the future with the forecasted warming trends of climate change requiring increased water supply for crop growth (Hughes 2003).

Chapter 4: Conclusions

This thesis investigated an approach for estimating transpiration fluxes at the catchment-level. The approach was applied to two case studies, the Gwydir and Namoi catchments in Northern NSW Australia. The primary data was sourced from MODIS NDVI imagery in a series of calculations which required the calculation of ancillary data. First, the solar radiation parameters were estimated; R_s grids were then created in ESOCLIM and R_o was calculated using Roderick (1999). Monthly NDVI grids from the MODIS satellite imagery at monthly intervals for 2000-2004. Then the fPAR was estimated from the monthly NDVI grids to get monthly fPAR. R_d/R_s was estimated to yield e, then f and e were used to estimate monthly GPP by using a radiation use efficiency approach. The monthly GPP grids were used as inputs to estimate monthly transpiration fluxes from May 2000 to December 2004. Then the monthly transpiration fluxes were summed to yield annual catchment scale transpiration fluxes for 2001-2004.

Analysis of the MODIS NDVI data involved distinguishing soil, vegetation and water pixels to compare their spectral signatures. This process calibrated the fPAR from the NDVI. Descriptive statistics were calculated using the monthly fPAR surfaces to delineate cropland and non cropland pixels in the Gwydir and Namoi catchments. The mean, variance, standard deviation and COV were calculated for each monthly fPAR surface for each year from 2001-2004. Then individual pixel analysis was performed on the annual transpiration grids to compare the difference in transpiration fluxes between cropland and non cropland pixels. This was followed by comparing the annual transpiration fluxes across the Gwydir and Namoi catchments.

Spatial and temporal estimates of transpiration fluxes yield several important results.

Temporal estimates of annual of transpiration fluxes show characteristics of wet and dry years. Catchment scale estimates of transpiration fluxes defined areas of high and low transpiration fluxes with high transpiration fluxes for wet years and low transpiration fluxes for dry years. Transpiration fluxes also increased with elevation. Vegetation on southerly aspects had higher transpiration rates due to increased radiation received at the surface. Contrasts between cropland and non cropland transpiration fluxes were discernable. Higher annual transpiration fluxes were observed in non cropland pixels and lower annual transpiration fluxes occurred in cropland pixels. Intra-

annual and inter-annual patterns of transpiration fluxes were detected from the individual pixel analysis.

This research demonstrated that fine resolution MODIS satellite data can be used to estimate catchment scale transpiration fluxes based on a radiation use efficiency approach. While this research was able to demonstrate the feasibility of the approach, unfortunately, no independent data set was available to validate the estimated transpiration fluxes. Similarly, there was insufficient time within the constraints of the Masters degree to enable the catchment-level transpiration fluxes to be analysed in conjunction with the rainfall and stream gauge data for the two case study catchments. Thus, I was unable to estimate the absolute or even relative contribution of transpiration to water balance in the case study catchments. Both these tasks should be the focus of future research.

4.1 Limitations and assumptions of study

Using satellite data to model vegetation parameters requires assumptions that can increase uncertainty and bias in the results. It is challenging to represent landscapes digitally since each individual study may focus on specific and different aspects of the land surface. The world we live in is heterogeneous and is functional at multiple scales (i.e. planet, continent, region, landscape, local ecosystem) which induce uncertainty in the digital representations of landscapes, as representations at one scale may not be useful at another. According to Longley *et al.* (2005) uncertainty can be defined as '*a measure of the user's understanding of the difference between the contents of a dataset and the real phenomena that the data are believed to represent.*' Spatial data is essentially a representation of the real world or a model of the landscape. Spatial modelling allows the user to alter the scale at which the observer perceives the landscape, and remotely sensed data differs in the spatial, temporal and spectral scales at which they sample the energy reflected/emitted from the land surface. Scaling problems can result in analysing processes by using information from one scale and applying that information to another scale (Raupach 1995).

It is generally difficult to represent the complexity of land cover data when using satellite data and particularly in the case of transpiration when the fundamental functional unit is a leaf and at the catchment level the leaf arrangements in a canopy; both of which vary at sub-pixel scales. A vegetation canopy therefore encompasses structural complexities which affect the way the satellite senses the object. fPAR depends on canopy characteristics such as differences in optical properties of evergreen

vegetation canopy and croplands, foliage clumping and leaf angle distribution. Due to this heterogeneity, the fPAR is likely to be underestimated by satellite-based sensors because of the scattering from the various leaf angles. Another limitation is that satellite images are taken at certain times of the day. The time of day affects the way light is reflected off of the canopy surface and is received by the sensor.

In this research it was assumed that the diffuse component of total radiation is the same throughout time (ESOCLIM estimates and Roderick 1999 calculation) when in reality the amount of radiation received at the surface is constantly changing. It is also assumed that fPAR and NDVI have a linear relationship when the relationship is actually near linear. There are several limitations of NDVI which in turn affect the estimates of fPAR. These include: external effects caused by atmosphere, clouds, aerosols, sun angle, ground contamination, structural and optical properties of the vegetation canopy. (Heute *et al.* 1994; Myneni *et al.* 1992; Myneni *et al.* 1995). Despite these limitations, remote sensing has been shown in other studies to be a non destructive, relatively accurate and cost-efficient way of measuring large scale dynamic canopy processes through time.

Catchment scale research integrates complex concepts such as scaling issues, modelling and process understanding. This research presents and investigated a new approach to estimating catchment scale transpiration fluxes. The estimated time-series values of transpiration can be readily integrated into catchment water balance process-based models. Estimates of catchment scale transpiration fluxes have important implications for catchment management in that it provides an explicit functional link between land use/land cover change and catchment-level water budgets. Monitoring transpiration fluxes could provide insight into how land use change (forest to cropland) alters catchment hydrology. In addition to quantifying the role of transpiration in the hydrologic cycle, catchment scale estimates of transpiration fluxes are useful in monitoring the state and productivity of agricultural crops, observing the spatial arrangement of transpiration fluxes across catchments, observing differences in transpiration fluxes for contrasting vegetation types, and monitoring changes in water use efficiency of different vegetation types (e.g. forest versus cropland).

Additional research on this topic could be extended to include other processes in the hydrologic cycle. For example, using satellite derived vegetation parameters and transpiration flux estimates with point based estimates of rainfall and stream flow data to create a catchment water balance model. This information could then be used to

determine if a catchment is energy limited or water limited. Catchment water balance research is essential in understanding the hydrological role of vegetation. Satellite data provides a reliable data source in which to further assess the impacts of drought conditions on vegetation productivity in water-limited environments across a range of scales. Water scarcity and allocation are bound to become some of Australia's major environmental issues in the coming years increasing the importance of integrated catchment management. The results of this thesis suggest an approach which could be used to better integrate vegetation as a component of catchment water balance calculations, help monitor natural resource management activities, and assist in the implementation of catchment management plans.

References

Anthes, R.A., 1984. Enhancement of convective precipitation by mesoscale variations in vegetative covering in semiarid regions, *Journal of Climate and Applied Meteorology*, 23: 541-554.

Asrar, G., Fuchs, M., Kanemasu, E.T. and Hatfield, J.L., 1984. Estimating absorbed photosynthetic active radiation and leaf area index from spectral reflectance in wheat, *Agronomy*, 76: 300-306.

Asrar, G., Myneni, R.B. and Choudhury, B.J., 1992. Spatial heterogeneity in vegetation canopies and remote sensing of absorbed PAR: a modelling study, *Remote Sensing of Environment*, 41: 85-103.

Australian Government (AG), 2004a. *Border Rivers-Gwydir Region Report Card*, Natural Resource Management, NSW. Available from: http://www.nrm.gov.au/state/nsw/border-rivers-gwydir/publications/report-card/index.html (Accessed 14 December 2005).

Australian Government (AG), 2004b. Namoi Region Report Card, Natural Resource Management, NSW. Available from:

http://www.nrm.gov.au/state/nsw/namoi/publications/report-card/ (Accessed 14 December 2005).

Barradas, V.L., Nicolas, E., Torrecillas, A. and Alarcon, J.J., 2005. Transpiration in young apricot (*Prunus armenica L.*) trees subjected to different PAR levels and water stress, *Agricultural Water Management*, 77(1-3): 323-333.

Barrett, D.J., Hatton, T.J., Ash, J.E. and Ball, M.C., 1996. Transpiration by trees from contrasting forest types, Australian Journal of Botany, 44: 249-263.

Barry, R.G. and Chorley, R.J., 1998. *Atmosphere, Weather and Climate*, (7th ed.). Routledge, London.

Beck, P.S.A., Atzberger, C., Hødga, K.A., Johansen, B. and Skidmore, A.K., 2005. Improved monitoring of vegetation dynamics at very high latitudes: a new method using MODIS NDVI, *Remote Sensing of Environment*, in press.

Berry, S.L., Farquhar, G.D., and Roderick, M.L., 2005. Co-evolution of climate, vegetation, soil and air, in *Encyclopedia of Hydrological Sciences*, ed M.G. Anderson, John Wiley & Sons, pp. 177-192.

Berry, S.L. and Roderick, M.L., 2002. Estimating mixtures of leaf functional types using continental-scale satellite and climatic data, *Global Ecology & Biogeography*, 11: 23-39.

Berry, S.L and Roderick, M.L., 2004. Gross primary productivity and transpiration flux of the Australian vegetation from 1788 to 1988 AD: effects of CO_2 and land use change, *Global Change Biology*, 10: 1884-1898.

Bonan, G., 2002. *Ecological Climatology: concepts and applications*, Cambridge University Press, Cambridge.

Bradford, A.S. and Zhang, L., 2002. Application of a mean annual water balance model to the Murray-Darling Basin: past, present and future. In: T.R. McVicar, L. Rui, J. Walker, R.W. Fitzpatrick and L. Changming (eds.) *Regional Water and Soil Assessment for Managing Sustainable Agriculture in China and Australia*, ACAIR Monograph No. 84, 277-290.

Brutsaert, W., 1982. *Evaporation into the Atmosphere*, D. Reidel Publishing Company, Holland.

Budyko, M.I., 1974. Climate and Life, Academic Press, New York.

Bureau of Meterology (BOM), 2005. *Climate averages*. Available from: http://www.bom.gov.au (Accessed 5 September 2005).

Cowan, I.R., 1982. Regulation of water use in relation to carbon gain in higher plants. In: O.L. Lange, P.S. Nobel, C.B. Osmond, H. Zeigler (eds.) *Physiological Plant Ecology II: water relations and carbon assimilation*, Springer-Verlag, Berlin. pp. 589-613.

Cowan I.R. and Farquahar, G.D., 1977. Stomatal function in relation to leaf metabolism and environment. In: D.H. Jennings (ed.) *Integration of Activity in the Higher Plant*, Society for Experimental Biology, Cambridge University Press, Cambridge. pp. 471-505.

Crapper, P.F., Beavis, S.G. and Zhang, L., 1997. Climate and hydrology in the Namoi Catchment, A.D. McDonald and M. McAleer (eds.) *MODSIM 97 International Congress on Modelling and Simulation 8-11 December Vol. 1*, pp. 300-305.

Davie, T., 2003. *Fundamentals of Hydrology*. Routledge, London.

Department of Land and Water Conservation (DLWC), 1999. Stressed rivers assessment report: Gwydir catchment, DLWC, Sydney.

Department of Land and Water Conservation (DLWC), 2002a. Stressed rivers assessment report: Namoi catchment, DLWC, Sydney.

Department of Land and Water Conservation (DLWC), 2002b. Water quality in the Namoi catchment: 2000-2001, HO/10/02

Department of Water Resources New South Wales, 1992. Water resources of the Namoi valley....doing more with our water, 31pp.

Donaldson, S., 1997. Gwydir River Catchment, Report on land degradation and proposals for integrated management, Department of Land and Water Conservation, Sydney, 149pp.

Eldridge, D.J. and Freudenberger, D., 2005. Ecosystem wicks: woodland trees enhance water infiltration in a fragmented agricultural landscape in eastern Australia, *Austral Ecology*, 30(3): 336-347.

Environmental Protection Authority, 1994. *Preliminary regional environment improvement plan: northern tablelands*, NSW Environmental Protection Authority, Sydney.

Farmer, D., Sivapalan, M., and Jothityangkoon, C., 2003. Climate, soil, and vegetation controls upon the variability of water balance in temperate and semiarid landscapes: downward approach to water balance analysis, *Water Resources Research*, 39(2), article no. 1035.

Farrar, T.J., Nicholson, S.E. and Lare, A.R., 1994. The influence of soil type on the relationships between NDVI, rainfall, and soil moisture in semiarid Botswana. II. NDVI response to soil moisture, *Remote Sensing of Environment* 50: 121-133.

Fensholt, R., Sandholt, I. and Rasmussen, M.S., 2004. Evaluation of MODIS LAI, fAPAR, and the relation between fAPAR and NDVI in a semi-arid environment using *in situ* measurements, *Remote Sensing of Environment*, 91: 490-507.

Fohrer, N., Haverkamp, S., Eckhardt, K. and Frede, H.G., 2001. Hydrologic response to land use changes on the catchment scale, *Physics and Chemistry of the Earth Part B - Hydrology, Oceans and Atmosphere*, 26(7-8): 577-582.

Fu, B., Zhao, W., Chen, L., Liu, Z. and Lü, Y., 2005. Eco-hydrological effects of landscape pattern change, *Landscape and Ecological Engineering*, 1: 25-32.

Geoscience Australia (GA), 2004. *Vegetation - Post European Settlement (1988): product user guide.* Geoscience Australia, Canberra. Available from: http://www.ga.gov.au/image_cache/GA2985.pdf (Accessed 14 December 2005).

Giorio, P. and Giorio, G., 2003. Sap flow of several olive trees estimated with the heat-pulse technique by continuous monitoring of a single gauge, *Environmental and Experimental Botany*, 49(1): 9-20.

Greening Australia, 2003a. *Native Vegetation Management: a needs analysis of regional service delivery in New South Wales & Australian Capital Territory Gwydir*, Bushcare support 2003. Available from: http://www.greeningaustralia.org.au/NR/rdonlyres/D581AC37-E7FD-4AD5-9025-AA33372E8BDD/712/NSWACTGwydir.pdf (Accessed 12 December 2005).

Greening Australia, 2003b. *Native Vegetation Management: a needs analysis of regional service delivery in New South Wales & Australian Capital Territory Namoi*, Bushcare support 2003. Available from: http://www.greeningaustralia.org.au/NR/rdonlyres/D581AC37-E7FD-4AD5-9025-AA33372E8BDD/713/NSWACTNamoi.pdf (Accessed 12 December 2005).

Guide to Australia: search for latitude and longitude of cities, Charles Sturt University, Australia, 2005. Available from: http://life.csu.edu.au/geo/findlatlong.html (Accessed 23 August 2005).

Gwydir Catchment Management Board (GCMB), 2003. Gwydir Catchment Blueprint: a blueprint for the future, NSW Department of Land and Water Conservation. 50pp.

Herrmann, S.M., Anyamba, A., and Tucker, C.J., 2005. Recent trends in vegetation dynamics in the African Sahel and their relationship to climate, *Global Environmental Change*, 15: 394-404.

Huemmrich, K.F. and Goward, S.N., 1997. Vegetation canopy PAR absorptance and NDVI: an assessment for ten tree species with the SAIL model, *Remote Sensing of Environment*, 61: 254-269.

Huete, A., Justice, C. and Liu, H., 1994. Development of vegetation and soil indices for MODIS-EOS, *Remote Sensing of Environment*, 49: 224-234.

Hughes, L., 2003. Climate change and Australia: Trends, projections and impacts, *Austral Ecology*, 28(4): 423-443.

Jarvis, P.G., 1981. Stomatal conductance, gaseous exchange and transpiration, in *Plants and their Atmospheric Environment*, eds J. Grace, E.D. Ford and P.G. Jarvis, Blackwell Scientific Publications, Oxford, pp. 175-204.

Justice, C.O., Vermote, E., Townshend, J.R.G., Defries, R., Roy, D.P., Hall, D.K., Salomonson, V.V., Privette, J.L., Riggs, G., Strahler, A., Lucht, W., Myneni, R.B., Knyazikhin, Y., Running, S.W., Nemani, R.R., Wan, Z., Huete, A., van Leeuwen, W., Wolfe, R.E., Giglio, L., Muller, J.P., Lewis, P. and Barnsley, M.J., 1998. The moderate resolution imaging spectroradiometer (MODIS)

: land remote sensing for global change research, *IEEE Transactions on Geoscience and Remote Sensing*, 36(4): 1228-1249.

Kerkhoff, A.J., Martens, S.N., Shore, G.A., and Milne, B.T., 2004. Contingent effects of water balance variation on tree cover density in semiarid woodlands, *Global Ecology and Biogeography*, 13: 237-246.

Kumar, M. and Monteith, J.L., 1982. Remote sensing of plant growth, in *Plants and the Daylight Spectrum*, ed H. Smith, Academic Press, London, pp. 133-144.

Lampert, G. and Short, A., 2004. Namoi River Styles Report, DIPNR, Available from: http://www.namoi.cma.nsw.gov.au/pdf/namoi_4_18.pdf (Accessed 5 September 2005).

Larcher, W., 2003. *Physiological Plant Ecology*, Springer-Verlag, Berlin.

Lillesand, T.M. and Keifer, R.W., 1994. *Remote Sensing and Image Interpretation*, Wiley & Sons, New York.

Linacre, E. and Geerts, B., 1997. *Climates & Weather Explained.* Routledge, London.

Longley, P.A., Goodchild, M.F., Maguire, D.J. and Rhind, D.W., 2005. *Geographic Information Systems and Science*, Wiley & Sons: England.

Maselli, F., Chiesi, M. and Bindi, M., 2004. Multi-year simulation of Mediterranean forest transpiration by the integration of NOAA-AVHRR and ancillary data, *International Journal of Remote Sensing*, 25(19): 3929-3941.

McCloy, K.R. and Lucht, W., 2004. Comparative evaluation of seasonal patterns in long time series of satellite image data and simulations of a global vegetation model, *IEEE Transactions on Geoscience and Remote Sensing*, 42(1): 140-153.

McNaughton, K.G. and Jarvis, P.G., 1983. Predicting the effects of vegetation changes on transpiration and evaporation, in: *Water Deficits and Plant Growth Vol. 7.*, Academic Press, New York. pp. 1-48.

MODIS atmosphere web, 2006. Available from:

http://modis-atmos.gsfc.nasa.gov/NDVI/index.html (Accessed 30 January 2006).

MODIS web, 2005. Available from: http://modis.gsfc.nasa.gov/ (Accessed 18 August 2005).

Monteith, J.L., 1972. Solar radiation and productivity in tropical ecosystems, *Journal of Applied Ecology* 9(3): 747-766.

Myneni, R.B. and Ganapol, B.D. and Asrar, G., 1992. Remote sensing of vegetation canopy photosynthetic and stomatal conductance efficiencies, *Remote Sensing of the Environment*, 42(3): 217-238.

Myneni, R.B., Keeling, C.D., Tucker, C.J., Asrar, G. and Nemani, R.R., 1997. Increased plant growth in the northern high latitudes from 1981-1991, *Nature*, 386: 698-702.

Myneni, R.B., Los, S.O. and Asrar, G., 1995. Potential gross primary productivity of terrestrial vegetation from 1982-1990, Geophysical Research Letters, 22(19): 2617-2620.

Namoi Catchment CD ROM, 2000. Water Information System for the Environment: database for rivers and wetlands.

Namoi Catchment Management Authority (NCMA), 2003. Integrated Catchment Management Plan for the Namoi Catchment 2002: a blueprint for the future. Department of Land and Water Conservation, pp. 1-45.

Nepstad, D.C., de Carvalho, C.R., Davidson, E.A., Jipp, P.H., Lefebvre, P.A., Negreiros, G.H., Silva, E.D., Stone, T.A., Trumbore, S.E. and Vieira, S., 1994. The role of deep roots in the hydrological and carbon cycles of Amazonian forests and pastures, *Nature*, 372: 666-669.

New South Wales Environmental Protection Authority (NSW EPA), 1999. Water quality and river flow interim environmental objectives: Namoi River catchment, Guidelines for river, groundwater and water management committees, EPA, Sydney, EPA 99/51.

New South Wales Parks and Wildlife Service (NPWS), 2004. Available from:

http://www.nationalparks.nsw.gov.au/npws.nsf/Content/Coolibah_Black_Box_woodland_endangered (Accessed 27 October 2005).

Northwest Catchment Management Committee., 1996. The Namoi: a catchment to talk about. Namoi Catchment Planning Taskforce. 21pp.

Pielke, R.A., Avissar, R., Raupach, M., Dolman, A.J., Zeng, X.B. and Denning, A.S., 1998. Interactions between the atmosphere and terrestrial ecosystems: influence on weather and climate, Global Change Biology, 4(5): 461-475.

Ramanathan, V., Crutzen, P.J., Kiehl, J.T., and Rosenfeld, D., 2001. Aerosols, climate, and the hydrological cycle, *Science*, 294: 2119-2124.

Raupach, M.R., 1995. Vegetation-atmosphere interaction and surface conductance at leaf, canopy and regional scales, *Agricultural and Forest Meteorology*, 73: 151-179.

Roderick, M.L., 1999. Estimating the diffuse component from daily and monthly measurements of global radiation, *Agricultural and Forest Meterology*, 95: 169-185.

Roderick, M.L., Farquahar, G.D., Berry, S.L. and Noble, I.R., 2001. On the direct effect of clouds and atmospheric particles on the productivity and structure of vegetation, *Oecologia*, 129: 21-30.

Sellers, P.J., 1985. Canopy reflectance, photosynthesis and transpiration, *International Journal of Remote Sensing*, 6: 1335-1372.

Sellers, P.J., 1987. Canopy reflectance, photosynthesis and transpiration: 2. the role of biophysics in the linearity of their independence, *Remote Sensing of Environment*, 21: 143-183.

Shukla, J. and Mintz, Y., 1982. Influence of land-surface evapotranspiration on the Earth's climate, *Science*, 215(19): 1498-1501.

Silberstein, R.P. and Sivapalan, M., 1995. Modelling vegetation heterogeneity effects on terrestrial water and energy balances, Environment International, 21(5): 477-484.

Sokal, R.R. and Rohlf, F.J., 1995. *Biometry*, Freeman, New York.

Stephenson, N.L., 1990. Climatic control of vegetation distribution: the role of the water balance, *The American Naturalist*, 135(5): 649-670.

Stirzaker, R.J., Cook, F.J. and Knight, J.H., 1999. Where to plant trees on cropping land for control of dryland salinity: some approximate solutions, *Agricultural Water Management*, 39: 115-133.

Szilagyi, J., 2000. Can a vegetation index derived from remote sensing be indicative of areal transpiration?, *Ecological Modelling*, 127: 65-79.

Thorpe, M.R., 1978. Net radiation and transpiration of apple trees in rows, *Agriculture and Forest Meteorology*, 19: 41-57.

Tournebize, R. and Boistard, S., 1998. Comparison of two sap flow methods for the estimation of tree transpiration, *Annales Des Sciences Forestieres*, 55(6): 707-713.

Tucker, C.J., Fung, I.Y., Keeling, C.D. and Gammon, R.H., 1986. Relationship between atmospheric CO2 variations and a satellite-derived vegetation index, Nature, 319: 195-199.

Veroustraete, F., Patyn, J. and Myneni, R.B., 1996. Estimating net ecosystem exchange of carbon using the normalized difference vegetation index and an ecosystem model, *Remote Sensing of Environment*, 58: 115-130.

Walker, J., Veitch, S., Braaten, R., Dowling, T., Guppy, L., Herron, N., 2001. Assessment of catchment condition in Australia's intensive land use zone: a biophysical assessment at the national scale, Final report Project 7/8 NLWRA. Available online: http://www.affa.gov.au/catcon/

Wilson, K.B., Hanson, P.J., Mulholland, P.J., Baldocchi, D.D. and Wullschleger, S.D., 2001. A comparison of methods for determining forest evapotranspiration and its components: sap-flow, soil water budget, eddy covariance and catchment water balance, *Agricultural and Forest Meteorology*, 106: 153-168.

Wullschleger, S.D. and Hanson, P.J., 2005. Sensitivity of canopy transpiration to altered precipitation in an upland oak forest: evidence from a long-term field manipulation study, *Global Change Biology*, 11: 1-13.

Zhang, H., Simmonds, L.P., Morison, J.I.L. and Payne, D., 1997. Estimation of transpiration by single trees: comparison of sap flow measurements with a combination equation, *Agricultural and Forest Meteorology*, 87: 155-169.

Zhang, L., Dawes, W.R. and Walker, G.R., 2001. Response of mean annual evapotranspiration to vegetation changes at catchment scale. *Water Resources Research*, 37(3): 701-708.

Appendices

METADATA

MODIS

Acquired from Dr Sandy Berry sandy.berry@anu.edu.au

MODIS_2000: 17 layers

Spatial extent

Top: -27.998875772906

Left: 145.99887577290599

Right: 154.00112422799802

Bottom: -32.001124227546001

Uncompressed file size: 205.41 MB

Datum: D_Clarke_1866

MODIS_2001: 23 layers

MODIS_2002: 23 layers

MODIS_2003: 23 layers

MODIS_2004: 23 layers

Spatial extent

Top: -27.998875772906

Left: 145.99887577290599

Right: 154.00112422799802

Bottom: -32.001124227546001

Uncompressed file size: 277.91 MB

Datum: D_Clarke_1866

Vegetation - post European settlement (1988)

http://www.ga.gov.au/meta/ANZCW0703005426.html

Dataset citation

ANZLIC unique identifier: ANZCW0703005426

Title: Vegetation - Post-European Settlement (1988)

Custodian

Custodian: Geoscience Australia

Jurisdiction: Australia

Description

Abstract:

Shows vegetation of Australia in the mid 1980s. Areas over 30 000 hectares are shown plus small areas of significant vegetation such as rainforest and croplands. Attribute information includes growth form of the tallest and lower stratum, foliage cover of tallest stratum and dominant floristic type.

ANZLIC search words:

FLORA Native Mapping

VEGETATION Mapping

Spatial domain:

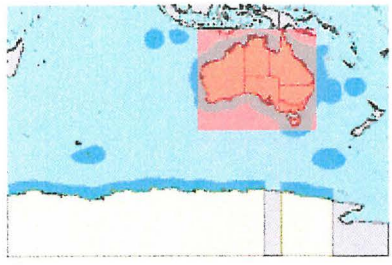

Geographic extent name: AUSTRALIA EXCLUDING EXTERNAL TERRITORIES - AUS - Australia - Australia

Note: The format for each Geographic extent name is: `Name - Identifier - Category - Jurisdiction` (as appropriate)

Geographic bounding box:

North bounding latitude: -9 °

South bounding latitude: -44 °

East bounding longitude: 154 °

West bounding longitude: 112 °

Data currency

Beginning date: Not Known

Ending date: 1985-01-01

Dataset status

Progress: Complete

Maintenance and update frequency: Not Known

Access

Stored data format:

DIGITAL - e00 ArcInfo export (e00) ArcInfo Workstation Geographic AGD66

DIGITAL - Map Printed map

Available format type:

DIGITAL - e00 ArcInfo export (e00) ArcInfo Workstation Geographic AGD66

DIGITAL - mif MapInfo Interchange Format (MIF) MapInfo Geographic AGD66

DIGITAL - shp ArcView shape file ArcView Geographic AGD66

DIGITAL - Map Printed map

Access constraints:

The data are subject to Copyright. Data files may be downloaded from Geoscience Australia's website at www.ga.gov.au/download/. A licence agreement is required.

Data quality

Lineage:

Captured from Geoscience Australia's 'Present Vegetation' 1:5 million scale map.

Positional accuracy:

Not Documented

Attribute accuracy:

Not Documented

Logical Consistency:

Not Documented

Completeness:

Complete for all Australia

Contact information

Contact organisation: Geoscience Australia (GA)

Contact position: Director, Sales and Distribution, CIMA

Mail address: GPO Box 378

Mail address:

Locality: Canberra

State: ACT

Country: Australia

Postcode: 2601

Telephone: +61 2 6249 9966

Facsimile: +61 2 6249 9960

Electronic mail address: sales@ga.gov.au

Metadata information

Metadata date: 2003-07-22

Additional metadata

Metadata reference XHTML: http://www.ga.gov.au/meta/ANZCW0703005426.html

Metadata reference XML: http://www.ga.gov.au/meta/ANZCW0703005426.xml

Size of database: 4.9 - 7.7 MB depending on the format.

Scale/resolution: 1:5 million